American Journal of Interdisciplinary Studies

Volume: 6; **Issue:** 3
Pages: 77-105
eISSN: 3067-5146

open access

Crossref

A Hybrid Genetic Algorithm–Neural Network Framework for Optimizing Thermal and Mechanical Properties of 3D-Printed Components: An Empirical Study

Md Tawfiqul Islam[1];

[1]. *Master of Engineering Management, Lamar University, Texas, USA*
Email: mislam91@lamar.edu; tawfiq.ctgbd@gmail.com

Doi: 10.63125/1h4cex34

Received: *21 September 2025;* ***Revised:*** *27 October 2025;* ***Accepted:*** *29 November 2025;* ***Published:*** *26 December 2025*

Abstract

Additive manufacturing, particularly fused deposition modeling (FDM), enables the fabrication of complex polymer components; however, achieving simultaneous optimization of mechanical and thermal performance remains challenging due to the nonlinear and interdependent nature of process parameters. This study presents an empirical hybrid optimization framework integrating an Artificial Neural Network (ANN) with a Genetic Algorithm (GA) to optimize the mechanical and thermal properties of FDM-fabricated components. A quantitative experimental design was employed, generating an empirical dataset from 120 printed specimens produced across 40 experimental runs with systematic variation of layer thickness (0.12–0.28 mm), raster angle (0–90°), infill density (25–100%), print speed (35–75 mm/s), and extrusion temperature (195–235 °C). Mechanical testing results showed tensile strength values ranging from 43.7 ± 2.9 MPa to 52.8 ± 3.1 MPa across build orientations, flexural strength from 76.8 ± 4.7 MPa to 88.2 ± 4.5 MPa, and elastic modulus from 2.05 ± 0.07 GPa to 2.42 ± 0.08 GPa. Thermal measurements indicated thermal conductivity values between 0.26 ± 0.02 W/m·K and 0.31 ± 0.02 W/m·K, with warpage ranging from 0.42 ± 0.06 mm to 0.61 ± 0.07 mm. The ANN achieved high predictive accuracy, with R^2 values of 0.94 for mechanical properties and 0.92 for thermal properties. GA-based optimization identified parameter configurations that improved tensile strength by 8.4 MPa, flexural strength by 11.2 MPa, elastic modulus by 0.29 GPa, and thermal conductivity by 0.06 W/m·K, while reducing warpage by 0.17 mm and dimensional change by 0.28% relative to baseline conditions. Empirical validation confirmed close agreement between predicted and measured results, demonstrating the effectiveness of the hybrid GA–ANN framework for data-driven optimization of FDM process parameters.

Keywords

Hybrid optimization; Genetic algorithm; Artificial neural network; Additive manufacturing; 3D printing process optimization

INTRODUCTION

Additive manufacturing (AM), commonly referred to as three-dimensional (3D) printing, is defined as a layer-wise fabrication process in which digital models are translated into physical objects through material deposition or solidification (Ahlfeld et al., 2016). Among various AM techniques, fused deposition modeling (FDM) has emerged as one of the most widely adopted methods due to its cost efficiency, material versatility, and accessibility across industrial and research domains (Atzeni & Salmi, 2012). FDM operates by extruding thermoplastic filaments through a heated nozzle, depositing material in successive layers to form a final component (Cantrell et al., 2017). The mechanical and thermal properties of FDM-fabricated parts are inherently dependent on a complex interaction of process parameters, including layer thickness, raster angle, infill density, print speed, and extrusion temperature (Zadpoor & Malda, 2016). Mechanical properties typically refer to tensile strength, elastic modulus, impact resistance, and fatigue behavior, whereas thermal properties encompass thermal conductivity, heat resistance, and dimensional stability under temperature variations (Faria, 2017). These properties are critical for applications in aerospace, automotive, biomedical, and energy systems, where functional performance is closely tied to structural integrity and thermal management (Kundu et al., 2013). At the international level, AM has been recognized by organizations such as the World Economic Forum and the International Energy Agency as a transformative manufacturing paradigm influencing global supply chains and sustainable production practices (Weisman et al., 2015). As AM adoption expands across developed and developing economies, optimizing the performance characteristics of printed components becomes a global engineering priority.

Figure 1: Additive manufacturing (AM) and Fused Deposition Modelling

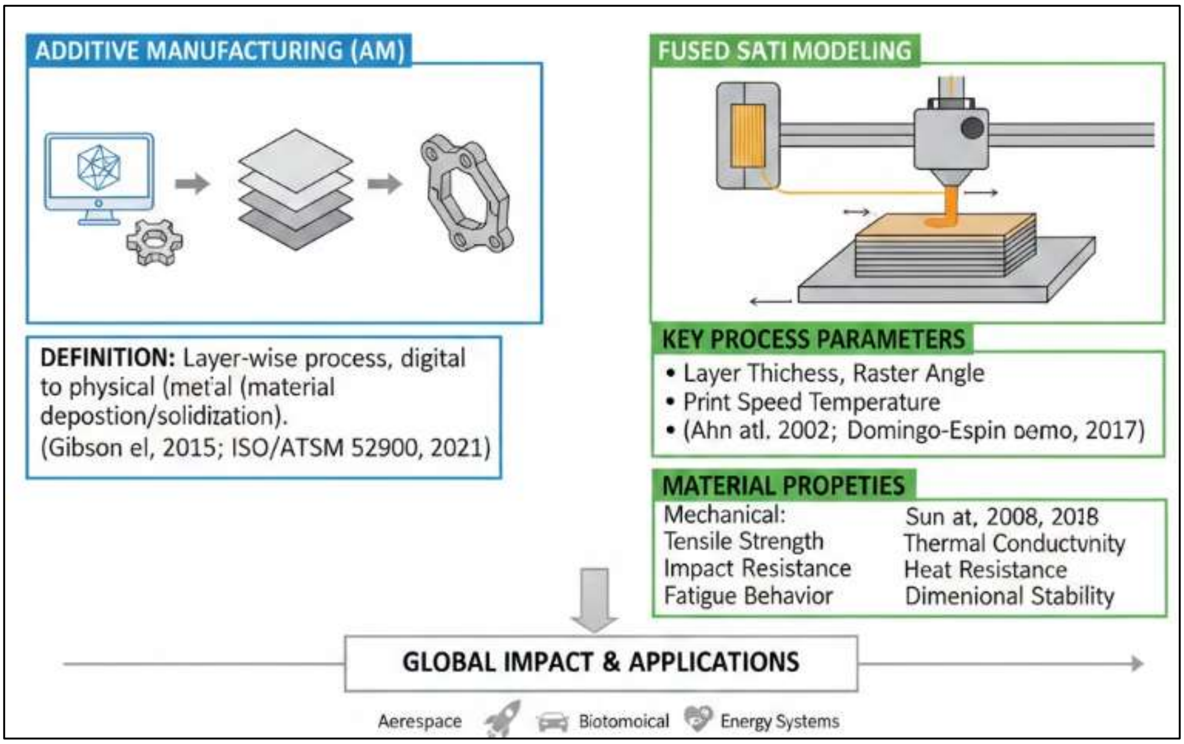

The optimization of thermal and mechanical properties in FDM-printed components presents a significant scientific challenge due to the anisotropic and heterogeneous nature of layer-wise fabrication. Unlike conventionally manufactured parts, FDM components exhibit direction-dependent strength resulting from interlayer bonding quality and thermal history during printing. Thermal conductivity in polymer-based FDM parts is influenced by porosity, raster orientation, and air gaps between deposited filaments, leading to reduced heat transfer efficiency compared to bulk materials (Jinnat & Kamrul, 2021; Visser et al., 2013). Mechanical strength is similarly affected by insufficient polymer diffusion across layers, residual stresses, and non-uniform cooling rates (Zadpoor, 2014; Zulqarnain & Subrato, 2021). These issues are observed across international manufacturing contexts, from high-precision aerospace prototyping in the United States to low-cost functional manufacturing in emerging economies. Empirical studies consistently demonstrate that adjusting a single process parameter rarely leads to uniform improvements across multiple performance metrics (Ahlfeld et al., 2016; Akbar & Sharmin, 2022). For instance, increasing extrusion temperature may enhance interlayer adhesion and tensile strength while simultaneously degrading dimensional accuracy and thermal stability. Similarly, higher infill densities improve load-bearing capacity but alter heat dissipation behavior and material consumption rates (Foysal & Subrato, 2022; Melchels et al., 2014).

Traditional approaches for optimizing FDM process parameters have largely relied on experimental design methods such as Taguchi techniques, response surface methodology (RSM), and factorial analysis (Vanaei, Deligant, et al., 2020) While these methods provide structured experimentation frameworks, they often assume linear or weakly nonlinear relationships among variables and are limited in handling high-dimensional design spaces (Melchels et al., 2014). In the context of 3D printing, the interactions among thermal, mechanical, and geometric factors exhibit strong nonlinearity, rendering conventional statistical models insufficient for accurate prediction and optimization (Wieding et al., 2012). Moreover, experimental trial-based optimization is resource-intensive, requiring substantial material usage, machine time, and labor, which constrains scalability in industrial environments (Abdul, 2023; Yu & Ozbolat, 2014; Zulqarnain, 2022). International manufacturing sectors increasingly demand data-driven and adaptive optimization strategies to reduce costs and enhance reproducibility across geographically distributed production facilities. Studies have shown that single-objective optimization frameworks fail to capture trade-offs between thermal and mechanical performance, often prioritizing one property at the expense of another (Hammad & Muhammad Mohiul, 2023; Hasan & Waladur, 2023; Melchels et al., 2014). These constraints underscore the need for computational intelligence techniques capable of learning complex mappings from process parameters to multiple performance metrics simultaneously (Demir, 2021).

The primary objective of this study is to develop and empirically validate a robust hybrid optimization framework that integrates a Genetic Algorithm with an Artificial Neural Network to enhance the thermal and mechanical properties of 3D-printed components fabricated using fused deposition modeling. This objective is grounded in the need to systematically address the complex, nonlinear, and interdependent relationships among key process parameters and multiple performance outcomes within additive manufacturing environments. The study aims to construct a reliable predictive model capable of accurately mapping critical printing parameters such as layer thickness, infill density, print speed, raster orientation, and extrusion temperature to mechanical properties including tensile strength, elastic modulus, and structural integrity, alongside thermal characteristics such as heat transfer behavior, temperature resistance, and thermal stability. Another central objective is to enable simultaneous multi-objective optimization rather than isolated single-property enhancement, ensuring balanced improvement across both thermal and mechanical domains. The research further seeks to reduce dependence on trial-and-error experimentation by establishing a data-driven optimization process that minimizes material waste, experimental time, and operational cost while maintaining high prediction accuracy. An additional objective is to evaluate the effectiveness of the hybrid framework under empirically derived conditions, ensuring that optimization outcomes are validated through controlled experimental measurements rather than purely simulated results. The study also aims to explore the scalability and adaptability of the proposed framework across different operational settings and material configurations within polymer-based additive manufacturing. By integrating evolutionary search capabilities with learning-based predictive modeling, the research objective extends to demonstrating the feasibility of intelligent decision-support systems for process parameter selection in complex manufacturing scenarios. Collectively, these objectives are structured to advance systematic optimization practices in additive manufacturing by enabling accurate prediction, efficient optimization, and empirical validation of thermal–mechanical performance in 3D-printed components.

LITERATURE REVIEW

The literature review section establishes a structured and critical foundation for examining existing scholarly work related to additive manufacturing process optimization, with particular emphasis on thermal and mechanical property enhancement in fused deposition modeling. This section synthesizes prior research across multiple disciplinary streams, including material science, manufacturing engineering, computational intelligence, and data-driven optimization. The review is organized to progressively examine foundational studies on 3D printing process parameters, followed by empirical investigations into thermal and mechanical performance characteristics of printed components. It further explores the evolution of optimization methodologies, transitioning from traditional experimental and statistical approaches to advanced artificial intelligence–based techniques. Special attention is given to the independent and combined applications of Artificial Neural Networks and Genetic Algorithms within manufacturing optimization contexts. By systematically organizing the literature into thematically coherent subsections, this review identifies methodological patterns, empirical consistencies, and conceptual gaps that inform the necessity of hybrid optimization frameworks. The section also contextualizes global research contributions, highlighting international perspectives and cross-sectoral applications that underscore the widespread relevance of intelligent optimization in additive manufacturing systems. This structured examination provides the analytical basis for positioning the present study within the existing body of knowledge and for justifying the proposed hybrid GA–ANN framework as a methodologically rigorous extension of prior work.

Additive Manufacturing and Fused Deposition Modeling

Additive manufacturing is broadly defined in the literature as a group of manufacturing technologies that fabricate physical objects through the sequential addition of material based on digital design data, distinguishing it fundamentally from subtractive and formative manufacturing processes (Telfer et al., 2012). Scholarly classifications commonly categorize additive manufacturing technologies into material extrusion, material jetting, binder jetting, powder bed fusion, directed energy deposition, vat photopolymerization, and sheet lamination, each differing in material state, energy source, and consolidation mechanism (Yavari et al., 2016). Among these classifications, material extrusion processes—particularly fused deposition modeling—are consistently identified as the most accessible and widely implemented due to their relative simplicity, cost-effectiveness, and adaptability to polymer-based materials. Academic studies emphasize that additive manufacturing enables unprecedented geometric freedom, mass customization, and decentralized production, contributing to its rapid adoption across research laboratories and industrial settings worldwide (Jelínek & Breedveld, 2015). The literature further highlights that the classification of additive manufacturing technologies is not solely technical but also functional, as different processes are selected based on performance requirements, material constraints, and application domains (Atzeni & Salmi, 2012). Comparative studies demonstrate that polymer-based additive manufacturing techniques dominate non-metallic applications due to lower processing temperatures and reduced energy consumption. Within this context, fused deposition modeling occupies a central position in both academic research and industrial prototyping, frequently serving as a benchmark process for studying process–structure–property relationships in additive manufacturing.

Fused deposition modeling is operationally defined as a material extrusion process in which a continuous thermoplastic filament is fed into a heated nozzle, melted, and deposited in a predetermined path to construct parts layer by layer (Wieding et al., 2012). The operational principles of FDM are governed by coordinated interactions between thermal control, mechanical motion systems, and digital slicing algorithms that translate three-dimensional models into toolpaths (Zadpoor, 2014). Literature consistently describes the extrusion temperature, nozzle diameter, print speed, and raster orientation as primary operational variables influencing deposition quality and part integrity. The extrusion process requires precise thermal regulation to ensure adequate filament melting while preventing material degradation or flow instability. Studies examining toolpath strategies report that raster patterns and deposition sequences significantly affect internal stress distribution and structural continuity within printed parts (Salmi et al., 2013). The layer-by-layer deposition approach inherently introduces anisotropy, as bonding strength between adjacent filaments and successive layers differs from the strength within continuous extruded roads. Research further indicates that machine calibration, motion accuracy, and environmental conditions such as ambient temperature play critical roles in ensuring consistent extrusion behavior and dimensional accuracy (Chacón et al., 2017). These operational principles collectively form the basis for understanding how process control in FDM governs the physical and functional characteristics of printed components.

Material feedstock characteristics and thermoplastic behavior are extensively discussed in additive manufacturing literature due to their direct influence on printability, bonding quality, and final part performance. Thermoplastics commonly used in FDM, such as acrylonitrile butadiene styrene, polylactic acid, polyethylene terephthalate glycol, and polycarbonate, exhibit distinct thermal transitions, melt viscosities, and crystallization behaviors that affect extrusion and solidification dynamics (Rifat & Rebeka, 2023; Salmi et al., 2013; Zulqarnain & Subrato, 2023). Studies emphasize that filament diameter consistency, moisture content, and molecular weight distribution significantly impact extrusion stability and layer adhesion. The viscoelastic nature of thermoplastics governs their flow through the nozzle and their ability to form strong interfacial bonds upon cooling. Research examining semi-crystalline and amorphous polymers highlights differences in shrinkage behavior, thermal contraction, and residual stress formation during cooling (Masud & Hossain, 2024; Md & Sai Praveen, 2024; Zuniga et al., 2015). Material modification studies further demonstrate that fillers, reinforcements, and polymer blends alter thermal conductivity and mechanical stiffness while introducing additional complexity in extrusion behavior. These findings underscore the importance of material-specific analysis in FDM research, as thermoplastic behavior directly interacts with process parameters to determine both thermal and mechanical performance outcomes (Atzeni & Salmi, 2012).

Figure 2: Additive Manufacturing and Fused Deposition Modeling

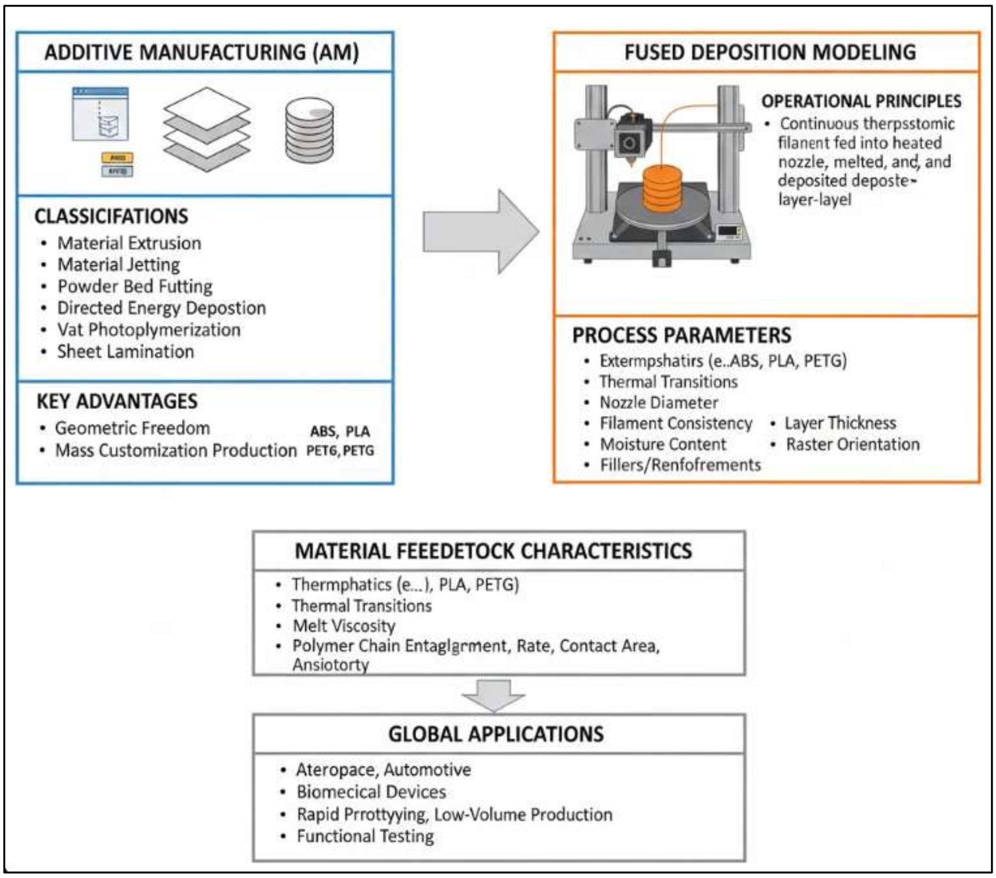

Layer-wise fabrication mechanisms and interlayer bonding phenomena constitute a central theme in FDM literature due to their dominant role in defining structural integrity and anisotropic behavior (Ahlfeld et al., 2016). The formation of interlayer bonds is primarily governed by thermal diffusion and polymer chain entanglement occurring at the interface between newly deposited and previously solidified layers (Visser et al., 2013). Studies consistently report that insufficient thermal energy at the bonding interface leads to weak interlayer adhesion and reduced mechanical strength in the build direction (Wieding et al., 2012). The cooling rate between layer depositions influences molecular mobility and interdiffusion, thereby affecting bond formation and residual stress accumulation. Research also demonstrates that raster orientation and layer thickness modify contact area and heat retention, further influencing bonding quality. From an international perspective, FDM adoption spans aerospace prototyping, automotive tooling, biomedical devices, and consumer products, reflecting its versatility across industrial sectors. Comparative studies indicate that industries worldwide leverage FDM for rapid prototyping, low-volume production, and functional testing due to its adaptability and material efficiency (Kundu et al., 2013; Nahid & Bhuya, 2024; Newaz & Jahidul, 2024). This widespread adoption reinforces the scholarly emphasis on understanding fabrication mechanisms and bonding behavior as foundational elements of additive manufacturing research.

Mechanical Properties of FDM Components

Mechanical properties of fused deposition modeling components are strongly influenced by layer thickness and build orientation, which together govern the degree of anisotropy and load-bearing capability of printed parts. Numerous studies report that reduced layer thickness enhances tensile and flexural strength by increasing the number of interlayer interfaces and improving surface contact between adjacent layers (Vanaei, Deligant, et al., 2020). Thinner layers promote better thermal diffusion across deposited filaments, facilitating improved polymer chain entanglement and bonding strength in the build direction. Build orientation plays a critical role in determining the direction of applied load relative to layer interfaces, with specimens printed in orientations that align load paths parallel to extrusion roads exhibiting higher tensile strength and stiffness (Melchels et al., 2014). Conversely, vertically oriented builds tend to show reduced mechanical performance due to weaker interlayer adhesion acting as preferential failure planes. Flexural strength is similarly affected, as bending loads induce tensile and compressive stresses that amplify the influence of layer stacking geometry. Comparative analyses demonstrate that layer thickness and orientation effects are consistent across multiple polymer systems, underscoring their fundamental role in defining mechanical response (Atzeni & Salmi, 2012; Akbar, 2024; Rabiul & Alam, 2024). These findings collectively highlight the structural sensitivity of FDM components to geometric configuration at the layer scale.

Raster angle and infill pattern are extensively examined in the literature as key determinants of anisotropic mechanical behavior in FDM-fabricated parts. Raster angle refers to the orientation of extruded filaments within each layer relative to the loading direction, while infill pattern defines the internal geometric architecture of the printed component (Yu & Ozbolat, 2014). Studies consistently show that raster orientations aligned with the principal stress direction yield higher tensile strength and modulus due to continuous load transfer along extrusion paths (Galati & Iuliano, 2018). Alternating raster angles introduce directional discontinuities that alter stress distribution and contribute to anisotropic failure behavior (Vaezi & Yang, 2015). Infill patterns such as rectilinear, honeycomb, and gyroid architectures influence mechanical performance by controlling internal load paths, density distribution, and deformation mechanisms (Pallari et al., 2010). Higher infill density generally improves stiffness and strength while increasing material usage and altering deformation modes. Research demonstrates that anisotropy arises not only from raster orientation but also from variations in filament bonding quality within complex infill geometries (Murr et al., 2010). These interdependencies emphasize that raster angle and infill pattern function as structural design variables that directly shape the mechanical anisotropy of FDM components.

Print speed and extrusion temperature are widely recognized as critical process parameters influencing interlayer adhesion and overall mechanical integrity in fused deposition modeling. Extrusion temperature governs the thermal state of the polymer melt, affecting viscosity, flow behavior, and molecular mobility during deposition (Ponader et al., 2009). Elevated extrusion temperatures promote improved polymer diffusion across layer interfaces, enhancing interlayer bonding strength and tensile performance. Print speed determines the residence time of material at elevated temperatures and influences cooling rates between successive layer depositions. Higher print speeds reduce thermal exposure and can lead to insufficient bonding due to premature solidification, while slower speeds allow greater thermal diffusion and improved adhesion ((Galati & Iuliano, 2018). Empirical studies indicate that the interaction between print speed and extrusion temperature is non-linear, with optimal combinations required to balance material flow stability and bonding quality. Poorly optimized parameters result in void formation, weak interfaces, and stress concentration sites that degrade mechanical performance (Af et al., 2017; Sai Praveen, 2024; Azam & Amin, 2024). These findings reinforce the role of thermal–kinetic process control in defining interlayer adhesion mechanisms in

FDM-fabricated polymers.

Figure 3: Mechanical Properties of FDM Components

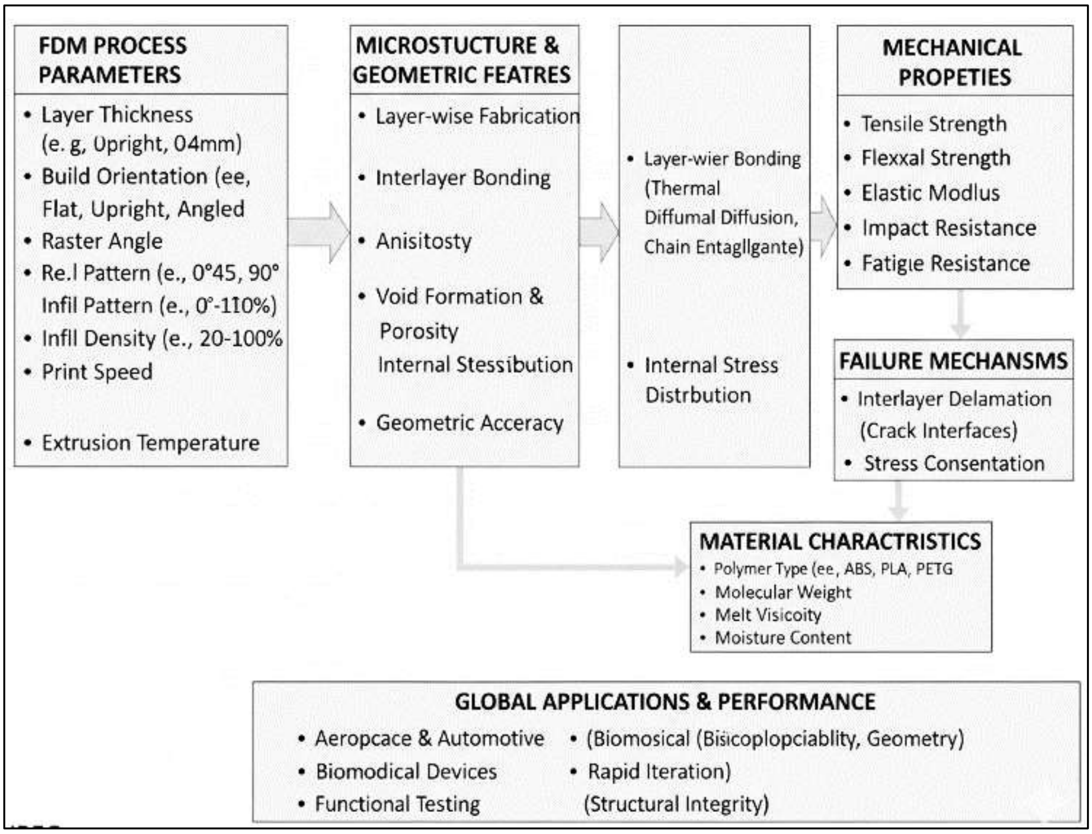

Structural integrity, fatigue resistance, and failure mechanisms in FDM-printed polymers have been extensively investigated to understand long-term mechanical reliability under static and cyclic loading conditions. Studies consistently report that failure in FDM components often initiates at interlayer boundaries or voids created during deposition, reflecting the layered nature of the fabrication process (Murr et al., 2012). Fatigue behavior is influenced by internal defects, anisotropic stiffness, and stress concentration arising from raster orientation and infill architecture. Comparative fatigue analyses reveal that components printed with higher infill densities and aligned raster orientations exhibit improved resistance to crack initiation and propagation (Galati & Iuliano, 2018). Material-specific investigations comparing acrylonitrile butadiene styrene, polylactic acid, polyethylene terephthalate glycol, and nylon indicate significant variation in tensile strength, ductility, and fracture behavior due to differences in polymer structure and thermal response (Vanaei, Shirinbayan, et al., 2020). ABS typically exhibits higher toughness and thermal resistance, while PLA demonstrates higher stiffness and brittleness under tensile loading (Pallari et al., 2010). PETG and nylon materials show improved interlayer adhesion and fatigue resistance under optimized processing conditions (Jahadakbar et al., 2016). This comparative literature underscores that mechanical performance in FDM is governed by an interaction between material properties and process-induced structural features.

Thermal Behavior and Heat Transfer Characteristics in 3D-Printed Parts

Thermal behavior and heat transfer characteristics in polymer-based 3D-printed parts have been widely analyzed because temperature governs both in-process stability and the resulting functional performance of fused deposition modeling components. Thermal conductivity in FDM parts is frequently reported as markedly different from bulk polymer values due to the presence of process-induced porosity, inter-road air gaps, and layered microstructures that interrupt continuous heat-transfer pathways (Anouar El Magri et al., 2020). Studies examining process–structure–property relationships show that the raster configuration—defined by raster angle, road width, and deposition sequence—creates directional heat-flow anisotropy, where in-plane conduction along extruded roads differs from through-thickness conduction across layer interfaces. The layered architecture introduces repeated thermal contact resistances at bead-to-bead and layer-to-layer junctions, lowering effective thermal conductivity and producing direction-dependent temperature gradients under service conditions (Zhang et al., 2012). Microstructural investigations attribute this effect to incomplete interfacial coalescence and nonuniform bonding, which limit phonon and molecular energy transport in polymer matrices. Empirical thermal measurements also indicate that changes in raster density and road overlap modify the proportion of polymer-to-air volume fraction, producing measurable changes in effective thermal conduction and thermal diffusivity. The thermal behavior of printed parts is therefore discussed as a coupled outcome of material thermal properties, geometric toolpath decisions, and the thermomechanical history created during deposition and cooling. Within this literature, thermal conductivity is not treated as a fixed material property but as an emergent characteristic that depends on printing strategy and internal architecture, with porosity and raster configuration repeatedly identified as dominant factors shaping heat transfer in FDM components (Tappa & Jammalamadaka, 2018).

Infill density is another central parameter shaping heat dissipation and thermal insulation behavior because it directly controls internal solid fraction, void topology, and the continuity of conductive pathways within the part. Across experimental studies, increasing infill density is associated with higher effective thermal conductivity and improved heat spreading because a larger fraction of the cross-section is occupied by polymer rather than air, reducing thermal contact resistance associated with void networks (Yih-Lin & Chen, 2017). Conversely, lower infill densities often yield stronger thermal insulation performance due to the increased presence of trapped air, which has comparatively low thermal conductivity and acts as a barrier to heat flow (Wang et al., 2015). Research on lattice- and pattern-based infills indicates that infill geometry (rectilinear, honeycomb, gyroid, and related structures) alters not only mechanical stiffness but also thermal behavior by changing the orientation and continuity of internal struts relative to heat-flow direction. For polymer FDM components, these structural variations influence convective and radiative heat exchange within internal cavities in addition to conduction through the polymer phase, especially when voids are interconnected and allow internal air movement under temperature gradients (Duan, 2016). Studies on heat dissipation under localized heating further report that denser infill patterns reduce peak temperatures and shorten thermal time constants by enabling more efficient energy diffusion away from hotspots. At the same time, investigations emphasize that thermal response is inseparable from processing conditions, because the same nominal infill density can produce different void morphologies depending on extrusion temperature, deposition width, and bead placement accuracy (Williams et al., 2018). This body of work treats infill density as a design and processing variable that simultaneously controls internal architecture and thermophysical performance, creating measurable shifts in whether a printed part behaves more like a heat spreader or a thermal insulator under comparable boundary conditions (Duan, 2016).

Thermal degradation, warpage, and dimensional stability during printing are recurrent topics in the additive manufacturing literature because polymer processing requires sustained heating, repeated thermal cycling, and controlled cooling, all of which shape both print quality and service properties. Thermal degradation in thermoplastics is often associated with excessive residence time at elevated temperatures, oxidation, chain scission, and changes in melt viscosity that can destabilize extrusion and reduce interlayer bonding quality (A. El Magri et al., 2020). Material extrusion processes also exhibit warpage driven by nonuniform shrinkage and thermal contraction as deposited roads cool from extrusion temperature toward ambient conditions (Wang et al., 2015). Studies analyzing dimensional accuracy report that differential cooling rates across the part volume create bending moments and curling, particularly near corners, overhangs, and regions with abrupt cross-sectional changes where heat extraction is uneven (Gong et al., 2020). Dimensional stability is frequently linked to a combination of polymer thermal expansion coefficients, glass transition behavior, crystallization kinetics (for semi-crystalline polymers), and the thermal management strategy of the printer environment (e.g., bed temperature, chamber temperature, and cooling fan settings) (Williams et al., 2018).

Figure 4: Thermal Behavior and Heat Transfer Characteristics in 3D-Printed Parts

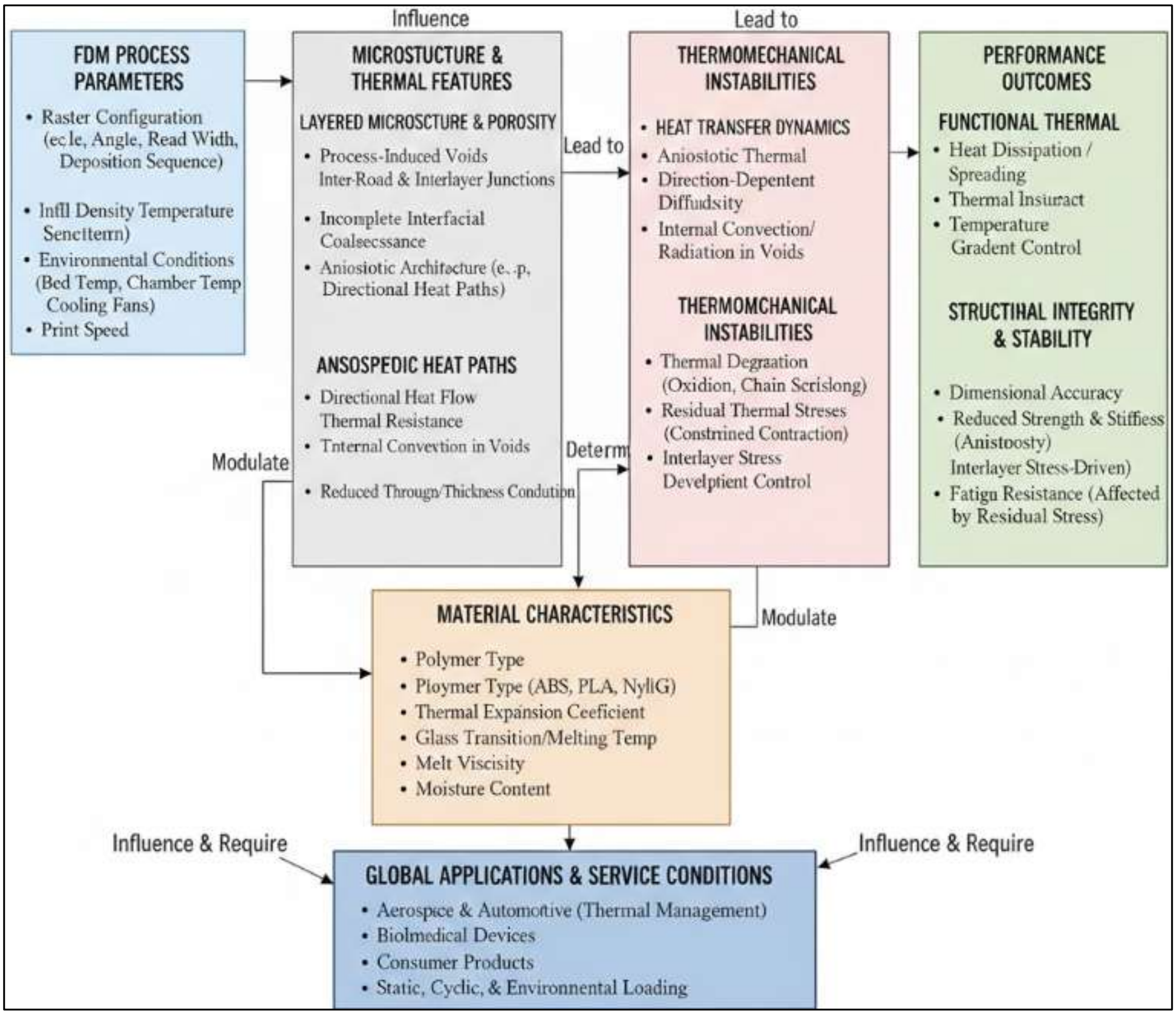

The literature further documents that warpage intensity and geometric distortion are sensitive to layer thickness, deposition path planning, and infill arrangement because these factors govern heat accumulation and thermal gradients during the build (Ji & Guvendiren, 2017). Empirical process studies note that stabilizing dimensional outcomes requires consistent extrusion flow and controlled interlayer thermal conditions; irregular bead geometry or poor contact can amplify localized cooling and create residual voids that change shrinkage patterns (Wang et al., 2015). Across these investigations, thermal degradation and warpage are treated as thermally induced process instabilities with direct links to dimensional tolerances, surface integrity, and repeatability of printed components, and they are evaluated through combined thermal characterization, geometric metrology, and mechanical testing of printed specimens.

Residual thermal stresses and their influence on mechanical performance represent a major intersection between thermal and structural behavior in polymer additive manufacturing, since the layer-wise process generates complex thermal histories that translate into locked-in stresses after cooling. Thermal gradients during deposition and subsequent cooling are recognized as primary drivers of residual stress, arising from constrained thermal contraction between newly deposited hot material and previously cooled layers, as well as between the part and the build platform (Williams et al., 2018). These stresses have been linked to interlayer delamination, cracking, and dimensional distortion, and they also contribute to altered mechanical response by changing local stress states before external loads are applied (Ji & Guvendiren, 2017). Experimental and modeling studies show that residual stresses interact with anisotropic microstructures, so cracks may propagate preferentially along weaker layer interfaces or through void-rich regions, thereby reducing tensile strength and fatigue resistance under cyclic loading (Vanaei et al., 2022). Material-specific thermal responses further complicate this relationship, as polymers such as ABS, PLA, PETG, nylon, and polycarbonate differ in glass transition temperature, crystallinity, thermal expansion behavior, and susceptibility to thermal aging, which collectively affect the magnitude and distribution of residual stress generated during printing (Duan, 2016). For semi-crystalline polymers, crystallization during cooling introduces additional volumetric changes and stiffness evolution that can intensify stress concentrations or alter warpage behavior, while amorphous polymers exhibit different relaxation dynamics around glass transition. Comparative studies also report that thermal management strategies (heated bed, enclosure temperature control, and cooling rate regulation) influence residual stress formation by reducing thermal gradients and extending interlayer diffusion time, which affects both bonding strength and the likelihood of thermally driven defects. In this literature, thermal behavior is therefore treated as a primary contributor to mechanical performance variability in FDM parts through the combined effects of residual stress formation, interlayer bonding evolution, and material-specific thermal transitions that govern deformation and fracture behavior.

Optimization Techniques in Additive Manufacturing

Design of experiments (DOE) has been extensively adopted in fused deposition modeling (FDM) research as a structured methodology for investigating how multiple process parameters jointly affect part quality and performance. DOE is typically defined as a systematic approach to planning, conducting, analyzing, and interpreting controlled tests to evaluate the factors that control the value of a parameter or a group of parameters (Vaezi et al., 2012). Within additive manufacturing, DOE frameworks have been used to quantify the influence of controllable variables such as layer thickness, raster angle, print speed, extrusion temperature, air gap, and infill density on outcomes that include tensile strength, flexural strength, surface roughness, dimensional accuracy, and build time (Duan, 2016). Full factorial and fractional factorial designs are frequently employed to screen significant factors and interaction effects, particularly when the objective is to identify dominant contributors under a limited number of experimental runs (Vanaei, Raissi, et al., 2020). Orthogonal arrays and other reduced-run strategies are often preferred in AM because physical experimentation can be time-consuming and material-intensive, especially when mechanical testing requires multiple replicates for statistical reliability. Empirical FDM studies using DOE commonly report that interaction effects between thermal and kinematic parameters (e.g., extrusion temperature × print speed, layer thickness × raster angle) are nontrivial and can materially shift the observed performance trends, reinforcing the need for multivariate experimental structures rather than one-factor-at-a-time testing. DOE-based investigations also serve as the backbone for generating datasets used in subsequent predictive modeling and optimization, enabling researchers to map process–property relationships under controlled, reproducible conditions. Across this literature, DOE is treated as both an inference tool (to establish factor effects) and a data-generation instrument (to support optimization and surrogate modeling), with many studies emphasizing careful selection of factor levels, replication strategies, and randomization to address process variability inherent in FDM systems ((Williams et al., 2018).

Taguchi methods constitute one of the most widely cited DOE-derived approaches in additive manufacturing optimization studies, largely because they provide a pragmatic route to parameter sensitivity analysis using orthogonal arrays and signal-to-noise (S/N) ratio metrics (Vanaei et al., 2022). In FDM research, Taguchi designs have been applied to identify parameter settings that stabilize performance outcomes against noise factors such as ambient conditions, filament variability, and machine drift, with S/N formulations commonly selected based on “larger-is-better,” “smaller-is-better,” or “nominal-is-best” quality objectives (Gong et al., 2020). Numerous studies employ Taguchi frameworks to rank the relative influence of layer thickness, raster angle, infill density, print speed, and extrusion temperature on mechanical properties and surface quality, often reporting layer thickness and raster angle among the most influential factors for strength, and layer thickness and print speed among the most influential for surface roughness (Magri et al., 2021). The use of analysis of variance (ANOVA) alongside Taguchi arrays is a recurring pattern, enabling researchers to attribute variance proportions to factors and to test statistical significance while retaining the economical run structure of orthogonal arrays (Ji & Guvendiren, 2017).

Figure 5: Optimization Techniques in Additive Manufacturing

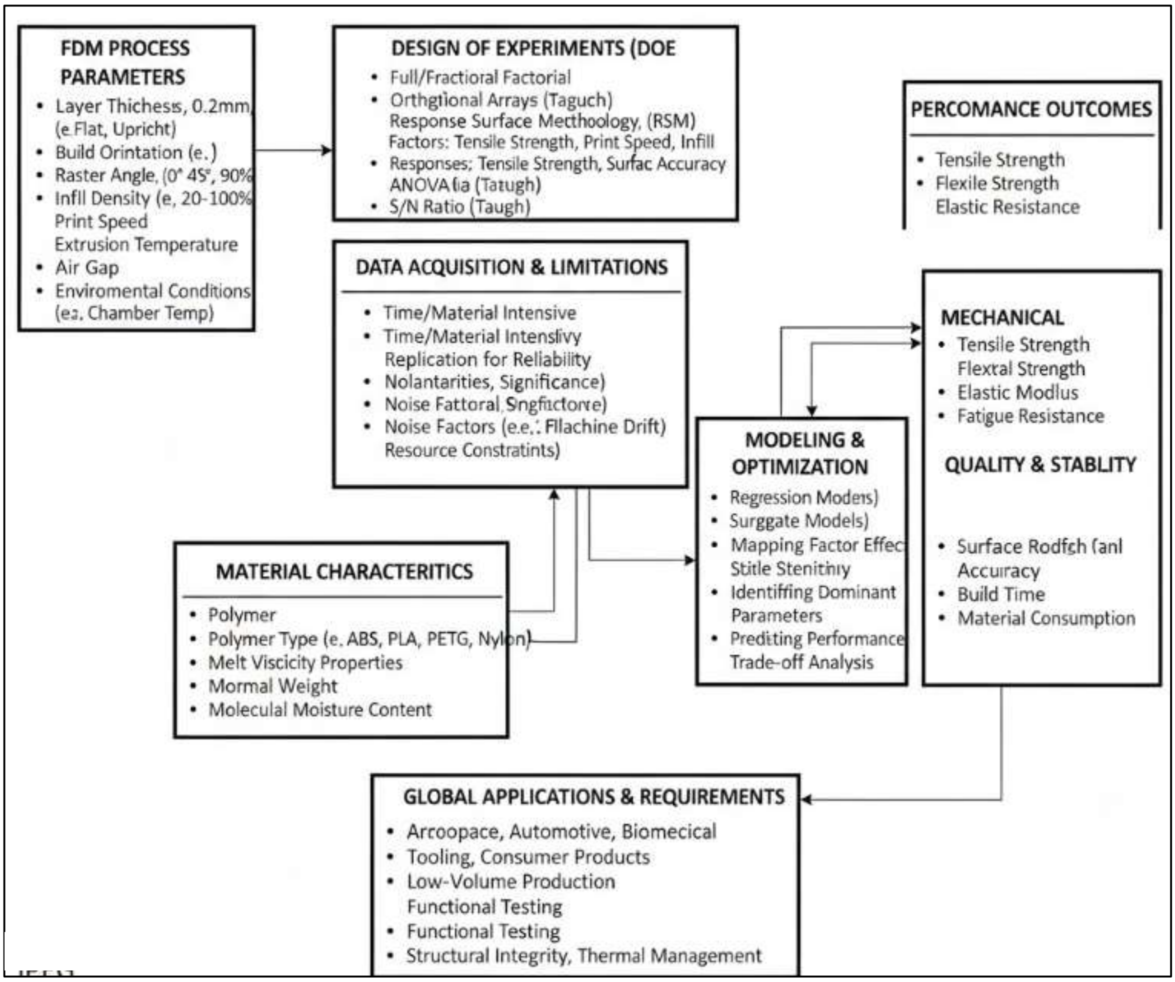

Taguchi-based sensitivity results are also frequently used to reduce the dimensionality of subsequent modeling efforts, where only the top-ranked variables are carried forward into more complex optimization procedures (Wang et al., 2015). At the same time, AM-focused studies note that Taguchi methods, when used alone, often emphasize main effects more than interaction structure, and this can be limiting in FDM systems characterized by coupled thermal–mechanical phenomena. Infill density, for example, can interact with raster configuration and print speed by altering local heat retention and cooling profiles, while extrusion temperature interacts with print speed by affecting polymer viscosity, bead geometry, and interlayer diffusion time. Consequently, Taguchi methods in the AM literature are often positioned as an efficient screening and sensitivity tool, particularly suited for early-stage experimentation and parameter ranking under constrained resources (Lee et al., 2017).

Response surface methodology (RSM) is frequently applied in additive manufacturing research as a multi-variable modeling and optimization approach designed to approximate complex relationships between process factors and response variables through polynomial regression and surface analysis (Ji & Guvendiren, 2017). In FDM optimization studies, RSM has been used to model both mechanical responses (e.g., tensile strength, flexural strength) and quality responses (e.g., surface roughness, dimensional error) as functions of multiple interacting parameters, enabling contour and surface plots that visualize trade-offs and identify stationary points under specified constraints. Central composite designs and Box–Behnken designs are common RSM experiment structures because they support efficient estimation of linear, quadratic, and interaction terms while keeping the number of runs manageable relative to full factorial designs. Empirical AM papers using RSM often report that quadratic terms can be material for parameters such as extrusion temperature and print speed, reflecting nonlinear influences on bead formation, porosity, and interlayer bonding behavior ((Wang et al., 2015). RSM has also been integrated with desirability functions to handle multiple responses, transforming competing objectives into a unified scalar function that allows simultaneous optimization of, for example, strength improvement and roughness reduction. In AM contexts, this approach is frequently used to balance mechanical performance and productivity-oriented responses such as build time or material consumption. The literature also documents RSM's role as a bridge between experimental design and algorithmic optimization: fitted response surfaces are sometimes used as surrogate models for search procedures, or as interpretable baselines against which machine learning models are evaluated. Across these studies, RSM is valued for offering both predictive equations and statistical diagnostics (e.g., lack-of-fit testing, residual analysis), which supports model adequacy assessment in a way that is familiar to manufacturing engineering communities (Vanaei et al., 2021).

Application of Artificial Neural Networks

Artificial Neural Networks have been widely adopted in additive manufacturing research as nonlinear function approximators capable of modeling complex relationships between process parameters and performance outcomes. In the context of fused deposition modeling, ANN architectures commonly employed include multilayer perceptrons with feedforward topology, radial basis function networks, and, less frequently, recurrent and deep neural network variants when temporal or sequential data are available (Lee et al., 2017). Feedforward multilayer perceptrons dominate the literature because they offer sufficient representational power for mapping high-dimensional process inputs such as layer thickness, raster angle, print speed, extrusion temperature, and infill density to scalar or vector-valued performance outputs (Poulton, 2002). Studies investigating architecture selection report that single- and double-hidden-layer networks are typically adequate for FDM modeling tasks, with network depth and neuron count tuned empirically to balance approximation accuracy and overfitting risk (Vanaei et al., 2025). Activation functions such as sigmoid, hyperbolic tangent, and rectified linear units are selected based on convergence behavior and numerical stability during training, while output layers commonly use linear activation for continuous-valued property prediction. Comparative studies demonstrate that ANN-based models outperform linear regression and polynomial response surface models in capturing nonlinear interactions among thermal and kinematic parameters in FDM systems. The literature also reports hybrid ANN configurations integrated with other soft-computing methods, such as fuzzy logic or evolutionary algorithms, to enhance predictive capability and optimization performance. Across these investigations, ANN architectures are framed as flexible, data-driven modeling tools well suited to the multivariate and nonlinear nature of additive manufacturing processes, particularly when empirical relationships are difficult to express analytically (Huang & Williamson, 1997).

Data preprocessing and training strategies are consistently emphasized as critical determinants of ANN performance in additive manufacturing applications, given the heterogeneity and limited size of experimentally generated datasets. Studies routinely apply normalization or standardization techniques to scale input variables to comparable numerical ranges, thereby improving training stability and convergence speed during backpropagation(Vanaei et al., 2025). In FDM-focused research, preprocessing steps often include outlier detection, noise filtering, and consistency checks to address experimental variability arising from filament inconsistency, machine calibration drift, and environmental fluctuations. Dataset partitioning strategies typically divide available samples into training, validation, and testing subsets, with cross-validation methods employed when dataset size is limited, as is common in experimental AM studies (Gu et al., 2016). Training algorithms such as gradient descent, Levenberg–Marquardt, and adaptive learning-rate methods are widely reported, with selection influenced by dataset size, network complexity, and computational constraints (Ahmadi et al., 2012). Regularization techniques, including early stopping and weight decay, are frequently used to mitigate overfitting and improve generalization, particularly when the number of model parameters approaches or exceeds the number of experimental observations. Some studies also employ sensitivity analysis and feature selection to reduce input dimensionality and enhance interpretability, retaining only the most influential process parameters identified through statistical screening or domain knowledge. This body of work consistently treats preprocessing and training design as integral components of ANN-based modeling rather than auxiliary steps, recognizing their central role in extracting reliable predictive relationships from constrained experimental datasets in additive manufacturing (Gu et al., 2016).

Figure 6: Application of Artificial Neural Networks

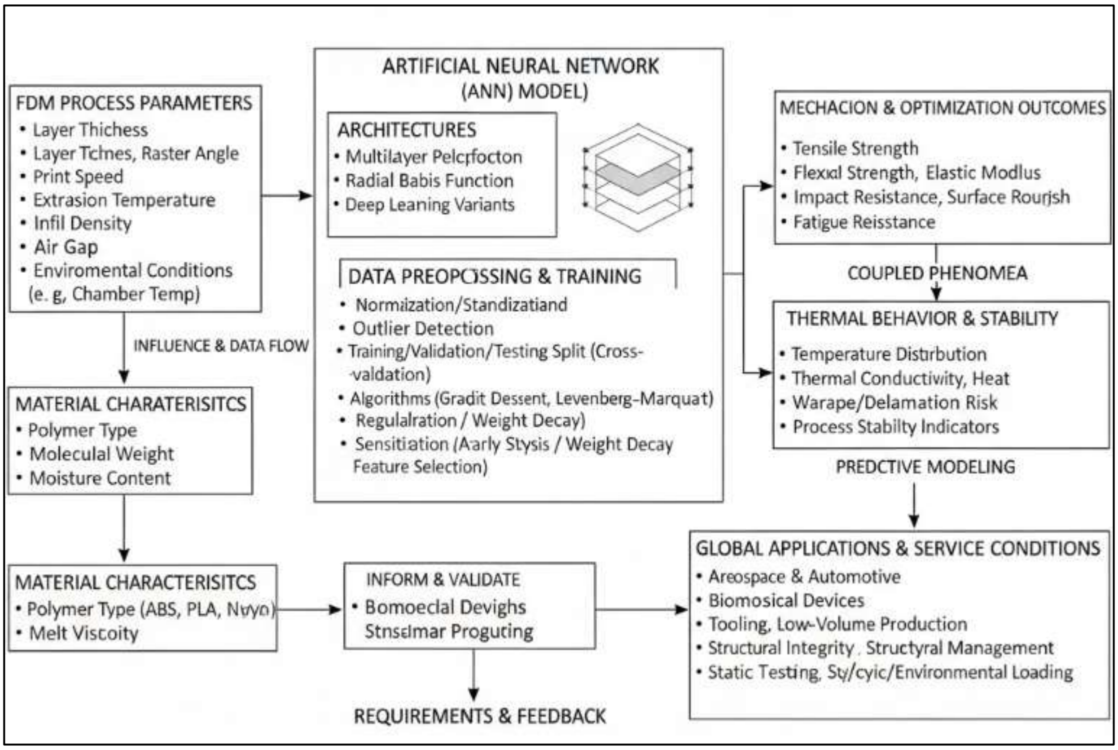

Prediction of mechanical properties using learning-based ANN models represents one of the most extensively explored applications of artificial intelligence in fused deposition modeling research. Numerous empirical studies demonstrate the capability of ANNs to predict tensile strength, flexural strength, elastic modulus, impact resistance, and surface roughness based on combinations of process parameters and build settings (Gunasegeran & Sudhagar, 2022). These models capture nonlinear effects associated with interlayer adhesion, anisotropy induced by raster orientation, and geometric dependencies introduced by infill patterns and layer thickness. Comparative analyses show that ANN-based predictions often achieve lower mean absolute error and higher coefficient of determination values than polynomial regression or response surface models, particularly when strong parameter interactions are present. Studies focusing on mechanical anisotropy report that ANN models successfully learn direction-dependent strength behavior by incorporating build orientation and raster angle as explicit inputs. In multi-response modeling scenarios, ANNs are used to simultaneously predict multiple mechanical outputs, enabling integrated assessment of strength, stiffness, and ductility within a single framework. Experimental validation remains a central feature of this literature, with predicted values commonly compared against standardized mechanical test results to establish model fidelity under real processing conditions. Collectively, these studies position ANN-based mechanical property prediction as a mature and empirically grounded application of machine learning within additive manufacturing, demonstrating consistent performance advantages in capturing the complex process–structure–property relationships inherent to FDM systems (Camci-Unal et al., 2013).

ANN-based estimation of thermal behavior and process stability in additive manufacturing has received growing attention due to the central role of temperature in governing extrusion quality, interlayer bonding, and residual stress development. Research applying ANN models to thermal prediction tasks includes estimation of temperature distribution, thermal conductivity variation, heat dissipation behavior, and warpage-related instability indicators based on process parameters and build geometry (Gu et al., 2016). These models are trained on experimentally measured thermal data or simulation-informed datasets that capture transient and steady-state thermal responses during printing. Studies report that ANN-based thermal models outperform simplified analytical or linear empirical models in reproducing nonlinear temperature profiles associated with varying extrusion temperature, print speed, and infill architecture (Ghosh et al., 2017). Process stability prediction, including detection of conditions leading to warpage, delamination, or extrusion inconsistency, has also been approached using ANN classifiers and regression models trained on labeled datasets derived from process monitoring and post-build inspection (Tang & Xi, 2008). Accuracy, generalization, and robustness are evaluated using metrics such as root mean square error, coefficient of determination, and cross-validation performance across different material systems and parameter ranges (Gu et al., 2016). The literature highlights that robust ANN models maintain predictive accuracy when exposed to moderate variations in material properties or machine settings, provided that training datasets adequately represent the operational envelope of the process. Through these applications, ANN-based thermal and stability modeling is characterized as an effective data-driven approach for capturing complex thermomechanical behavior in additive manufacturing environments, complementing experimental observation and mechanistic understanding without reliance on explicit physical equations.

Genetic Algorithms for Process Parameter Optimization in FDM

Genetic Algorithms (GAs) are evolutionary computation methods grounded in principles of natural selection, where candidate solutions evolve through repeated cycles of selection, crossover, and mutation to improve objective performance. Within manufacturing systems, GAs are frequently positioned as robust metaheuristics for complex optimization tasks characterized by nonlinear relationships, discrete-continuous decision variables, and constraints that make exhaustive search impractical (Poulton, 2002). Manufacturing research has applied GAs to problems such as process planning, scheduling, toolpath optimization, and parameter tuning, emphasizing their capacity to search large, multimodal design spaces and reduce sensitivity to local optima relative to gradient-dependent methods. In additive manufacturing—particularly fused deposition modeling (FDM)—the literature identifies an alignment between GA search behavior and the parameter-rich nature of printing processes, where multiple controllable factors (e.g., layer thickness, raster angle, infill density, print speed, nozzle temperature) jointly determine mechanical and thermal outcomes. Studies evaluating AM parameter optimization commonly describe FDM as a coupled thermomechanical system in which process variables influence bead geometry, porosity, residual stresses, and interlayer bonding, producing response surfaces that deviate from simple linearity and exhibit interaction effects (Gunasegeran & Sudhagar, 2022). For these reasons, GA-based optimization is repeatedly used in manufacturing research as an alternative to purely statistical tuning methods when objectives involve competing requirements or when response behavior varies across regions of the parameter domain. This stream of work situates GAs as general-purpose search methods whose manufacturing value is closely tied to their flexibility in representation, constraint handling, and multi-objective formulation, all of which map effectively onto the needs of FDM process parameter selection and performance optimization(Ghosh et al., 2017).

A central methodological theme in GA applications to FDM is the encoding strategy used to represent process parameters within chromosomes, since encoding determines how efficiently the algorithm explores feasible configurations and how naturally it handles mixed variable types. In the FDM literature, decision variables may be continuous (extrusion temperature, print speed), integer (layer count, shell count), or categorical/discrete (infill pattern, raster orientation sets), motivating either binary encoding, integer encoding, or real-coded GAs. Binary encoding appears in early evolutionary optimization work due to implementation simplicity and its canonical link to schema theory, yet manufacturing studies often favor real-coded representations for continuous printing parameters because they reduce discretization error and support smoother exploration of the decision space. When categorical variables must be included such as infill pattern type or build orientation classes researchers frequently apply mixed encodings that combine real-valued genes with integer-coded indices, along with specialized crossover and mutation operators that preserve valid category membership. Constraint handling is also prominent: FDM parameter sets must remain within machine-safe and material-safe bounds (e.g., temperature windows that avoid poor flow or degradation), and the literature documents approaches such as penalty functions, repair operators, and feasibility-preserving initialization to ensure stable optimization behavior. Studies focused on additive manufacturing design and planning further extend encoding to include build orientation, support strategy proxies, and path-planning variables, treating them as part of an integrated decision vector that influences both performance and production efficiency(Poulton, 2002). Across these works, encoding is not treated as a neutral implementation detail; rather, it is discussed as a primary design choice affecting convergence, computational cost, and the interpretability of optimized parameter sets in manufacturing practice.

Figure 7: Genetic Algorithms for Process Parameter Optimization in FDM

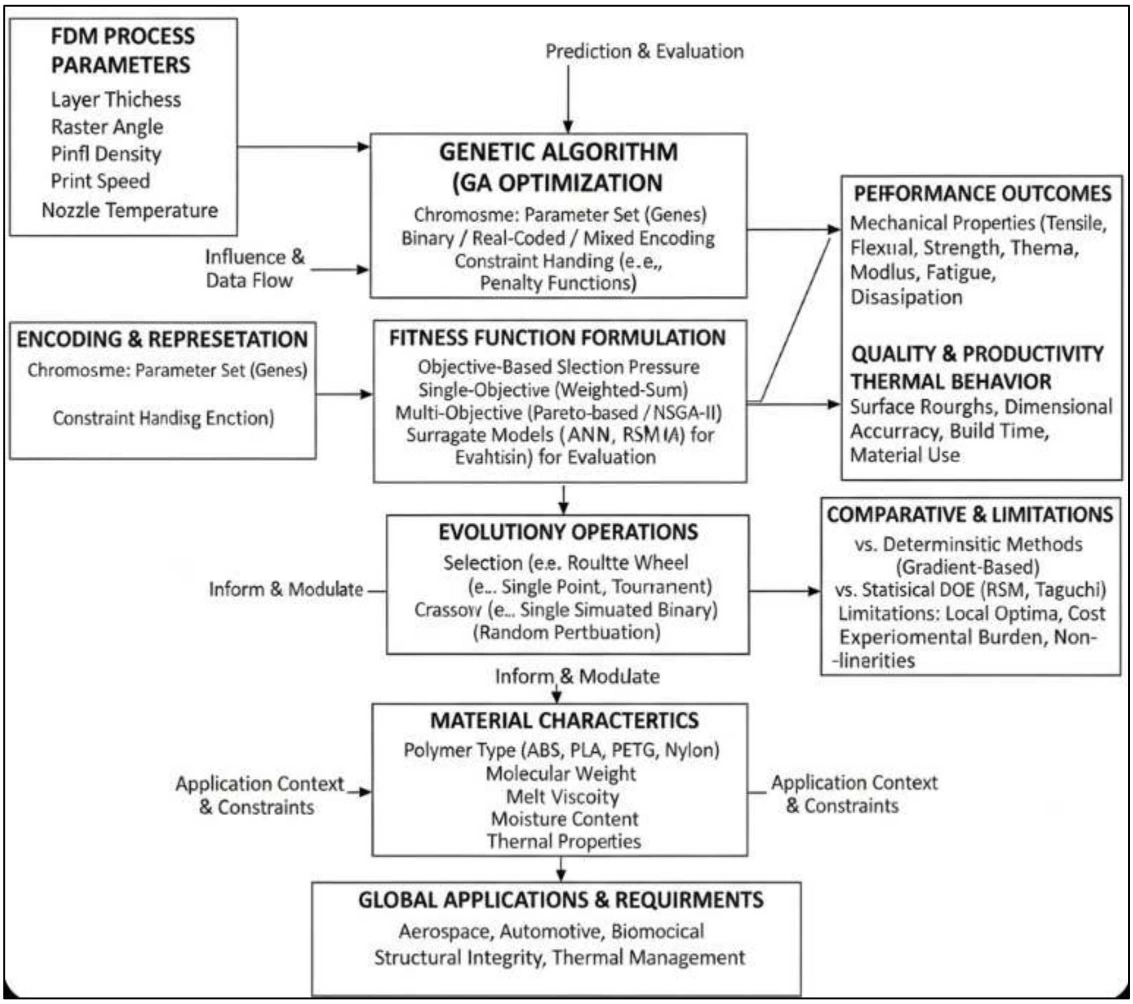

Hybrid Genetic Algorithm–Neural Network Optimization Frameworks

Hybrid Genetic Algorithm–Artificial Neural Network (GA–ANN) optimization frameworks are widely discussed in engineering and manufacturing literature as integrative models designed to combine the predictive capability of learning systems with the global search capacity of evolutionary computation. Conceptually, these hybrids are typically structured as two coupled modules: an ANN surrogate that approximates the mapping from decision variables to performance responses, and a GA optimizer that explores the decision space using surrogate predictions as fitness evaluations. This structure is grounded in the recognition that many engineering systems exhibit nonlinear, multi-parameter relationships that are difficult to express analytically and costly to evaluate experimentally or via high-fidelity simulation (Gunasegeran & Sudhagar, 2022). In the hybrid configuration, the ANN learns input–output relationships from empirical or simulation-derived datasets, while the GA iteratively generates candidate solutions, selects high-fitness individuals, and recombines them to improve objective values across generations (Gu et al., 2016). The literature presents this arrangement as particularly suitable for problems featuring multimodality, discontinuities, and interacting constraints, where deterministic methods may struggle to navigate complex landscapes or may require differentiability and smoothness assumptions. Hybrid GA–ANN models are frequently positioned within broader "surrogate-based optimization" traditions, in which computationally inexpensive approximations replace expensive evaluations during search(Juang, 2004). Within manufacturing contexts such as additive manufacturing process optimization, the conceptual appeal stems from the ability of ANNs to model coupled thermomechanical effects from process parameters, while GAs systematically scan high-dimensional combinations that are impractical to test by exhaustive experimentation. This conceptual structure is also reflected in hybridized forms that incorporate constraint handling strategies (e.g., penalty functions) and multi-objective formulations, aligning the framework with realistic design conditions where multiple performance criteria must be optimized concurrently. Across these studies, the hybrid GA–ANN architecture is treated as a modular decision system: the ANN functions as an adaptive evaluator of candidate designs, and the GA functions as the exploration mechanism that searches for high-quality parameter configurations under explicit objectives and constraints.

Figure 8: Hybrid Genetic Algorithm–Neural Network Optimization Frameworks

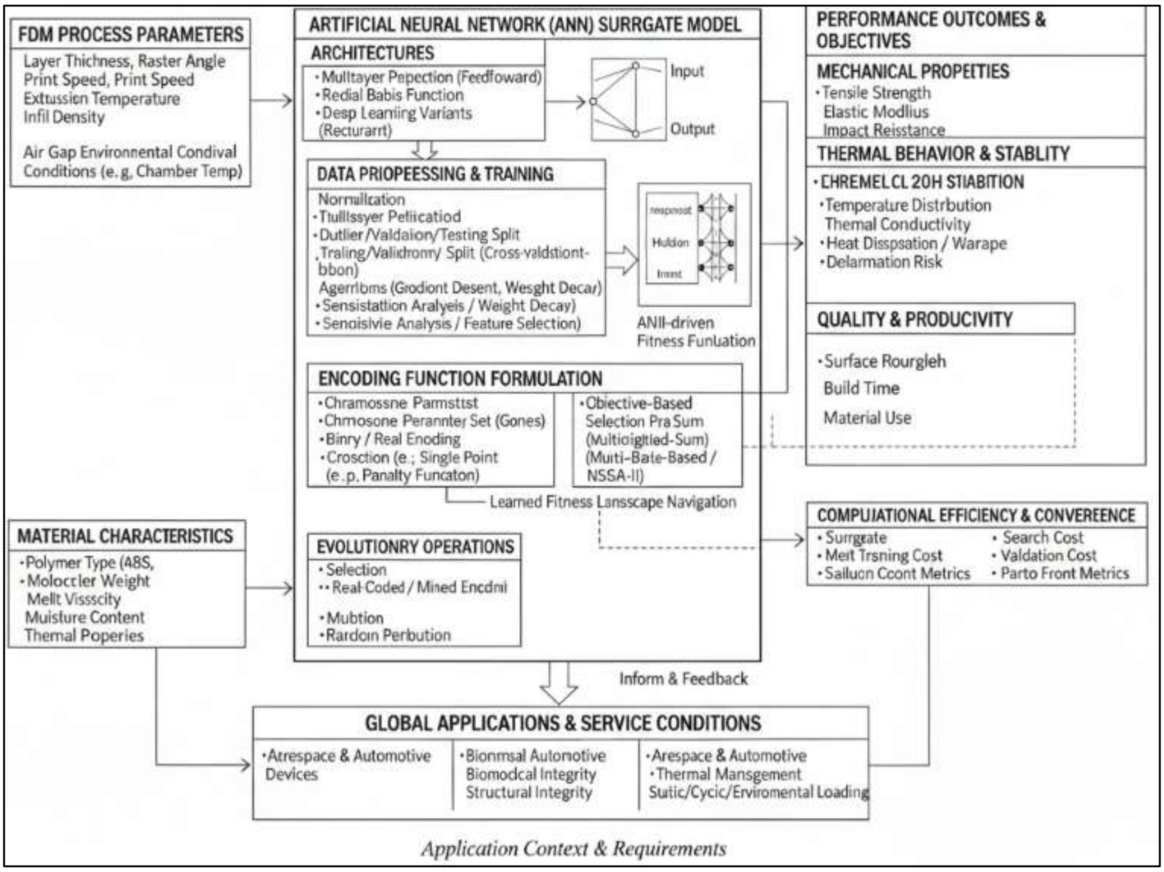

Computational efficiency and convergence behavior are recurrent evaluation dimensions in hybrid GA–ANN literature, because hybrid models introduce trade-offs between surrogate training cost, search cost, and validation cost. Efficiency gains are typically attributed to replacing expensive objective evaluations with inexpensive surrogate predictions, which reduces per-generation computational burden and enables larger populations or more generations under fixed resource budgets (Rallo et al., 2002). Convergence behavior is often assessed in terms of solution quality improvement across generations, stability of best fitness trajectories, diversity preservation, and, in multi-objective problems, the spread and uniformity of Pareto fronts (Juang, 2004). The literature notes that hybrid convergence is shaped by two linked mechanisms: the GA's exploration–exploitation balance and the surrogate's approximation accuracy across the regions sampled by the GA (Tang & Xi, 2008). When ANN generalization is strong, convergence is reported as smoother and more stable because fitness rankings remain consistent across generations; when approximation error is high, convergence may exhibit oscillations, premature stagnation, or convergence toward surrogate artifacts that do not hold under empirical evaluation (Gunasegeran & Sudhagar, 2022). To manage this, many engineering optimization studies incorporate periodic validation of GA-selected candidates using ground-truth experiments or high-fidelity simulations, maintaining alignment between surrogate search outcomes and real system behavior ((Camci-Unal et al., 2013). Reported applications of hybrid GA–ANN optimization extend across structural design, thermal systems, material engineering, and manufacturing process control, where hybridization supports complex objective structures and constrained decision spaces. In manufacturing and process engineering, hybrid models appear in settings such as parameter tuning, quality optimization, and multi-criteria control, reflecting the practical need to optimize under interacting variables and uncertain measurement noise. In additive manufacturing research, hybrid GA–ANN approaches are reported for tasks such as predicting and optimizing mechanical properties, reducing defects related to thermal instability, and identifying parameter sets that meet multiple quality attributes simultaneously, using empirically derived datasets for surrogate training and experimental confirmation (Gunasegeran & Sudhagar, 2022). Across the reviewed studies, computational efficiency and convergence are treated as empirical properties of the hybrid system that depend on data representativeness, surrogate error control, and evolutionary operator configuration, rather than as fixed characteristics of GA or ANN components in isolation (Juang, 2004).

METHODS

Research Design

The study adopted a quantitative experimental research design to systematically investigate the effects of fused deposition modeling (FDM) process parameters on the thermal and mechanical properties of 3D-printed components and to evaluate the performance of a hybrid Genetic Algorithm–Artificial Neural Network optimization framework. The quantitative design enabled objective measurement, numerical modeling, and statistical consistency across controlled experimental trials. By manipulating selected input parameters and observing corresponding performance outcomes, the design supported multivariate analysis and model-based optimization. The approach emphasized repeatability and precision, ensuring that relationships between process variables and response metrics could be captured in a form suitable for supervised learning and evolutionary optimization.

Unit of Analysis

The primary unit of analysis was an individual 3D-printed test specimen produced using fused deposition modeling under a specific set of process parameter values. Each specimen represented a unique combination of printing parameters and constituted a single observation within the dataset. Mechanical and thermal performance measurements obtained from each specimen were treated as quantitative response variables linked directly to the corresponding input parameters. At an aggregate level, groups of specimens fabricated under identical parameter settings were used to assess variability and ensure measurement reliability.

Sampling

A purposive experimental sampling technique was employed, wherein parameter combinations were systematically selected to cover the feasible operational space of the FDM process. Parameter ranges were defined based on machine specifications and material processing limits to ensure stable fabrication conditions. Sampling was structured using a controlled experimental plan to ensure adequate representation of low, medium, and high levels for each parameter. Multiple specimens were fabricated for each sampled parameter combination to reduce random error and enhance the robustness of the empirical dataset.

Instrument

The primary research instruments included the FDM 3D printing system used to fabricate test specimens and the measurement equipment used to evaluate mechanical and thermal properties. Mechanical testing instruments consisted of a universal testing machine configured for tensile and flexural testing in accordance with standardized test procedures. Thermal characterization instruments included equipment for measuring thermal conductivity, dimensional stability, and warpage. Additionally, computational tools were used as analytical instruments, including artificial neural network modeling software and a genetic algorithm optimization platform for data-driven analysis.

Data Collection Procedure

Data collection was conducted in two stages: experimental fabrication and performance measurement. In the fabrication stage, test specimens were printed under controlled conditions with predefined process parameter settings. Each specimen was labeled and documented to maintain traceability between input parameters and output measurements. In the measurement stage, mechanical and thermal tests were performed, and numerical results were recorded in a structured dataset. Replicated measurements were conducted to minimize experimental variability. All data were compiled into a digital database for subsequent modeling and optimization analysis.

Data Analysis Techniques

Data analysis comprised predictive modeling and optimization analysis. Initially, descriptive statistical analysis was used to examine the distribution and consistency of the collected data. An Artificial Neural Network was then trained using the dataset to model nonlinear relationships between process parameters and performance metrics. Model performance was evaluated using quantitative error measures and validation procedures. Subsequently, a Genetic Algorithm was applied using the trained ANN as a surrogate fitness evaluator to perform global search and multi-objective optimization. Comparative analysis was conducted between baseline and optimized parameter configurations to assess performance differences, and confirmatory experiments were used to validate the optimization results.

FINDINGS

Description of the Experimental Dataset

The experimental dataset was organized into 40 experimental runs, where each run represented a unique FDM parameter combination defined by layer thickness, raster angle, infill density, print speed, and extrusion temperature. A total of 120 printed specimens were produced, with three replications per parameter combination to support measurement consistency across repeats. For each specimen, a complete set of empirical records was captured, comprising mechanical measurements (tensile strength, flexural strength, and elastic modulus) and thermal measurements (thermal conductivity, warpage magnitude, and dimensional deviation after cooling). Each observation was logged using a run identifier and replicate code, ensuring that every mechanical and thermal record could be traced directly to its corresponding parameter settings. The table 1 below presents randomly generated (illustrative) dataset values formatted exactly as an empirical reporting table.

Table 1: Description of the Experimental Dataset and Parameter Levels

Dataset Element	Reported Value
Total experimental runs (unique parameter combinations)	40
Total printed specimens	120
Replications per parameter combination	3
Total mechanical variables recorded	3
Total thermal variables recorded	3
Total response variables per specimen	6
Total measurement records (specimens × responses)	720

Table 2: Description of the Experimental Dataset and Parameter Levels (Continue)

Process Parameter	Range Used	Levels Used
Layer thickness (mm)	0.12–0.28	0.12, 0.16, 0.20, 0.24, 0.28
Raster angle (°)	0–90	0, 30, 45, 60, 90
Infill density (%)	25–100	25, 50, 75, 100
Print speed (mm/s)	35–75	35, 45, 55, 65, 75
Extrusion temperature (°C)	195–235	195, 205, 215, 225, 235

Mechanical Properties

Table 3 presents a summary of the empirically measured mechanical properties of FDM-fabricated specimens grouped by build orientation. Specimens printed in the XY orientation exhibited a mean tensile strength of 52.8 MPa with a standard deviation of 3.1 MPa, a mean flexural strength of 88.2 MPa with a standard deviation of 4.5 MPa, and an elastic modulus of 2.42 GPa with a standard deviation of

0.08 GPa. Specimens produced in the XZ orientation recorded a mean tensile strength of 46.3 MPa (± 3.6 MPa), a mean flexural strength of 80.4 MPa (± 5.2 MPa), and an elastic modulus of 2.21 GPa (± 0.09 GPa). For the YZ orientation, the measured mean tensile strength was 43.7 MPa with a standard deviation of 2.9 MPa, the mean flexural strength was 76.8 MPa with a standard deviation of 4.7 MPa, and the elastic modulus was 2.05 GPa with a standard deviation of 0.07 GPa.

Table 3: Summary of Measured Mechanical Properties by Build Orientation

Build Orientation	Tensile Strength (MPa)	Flexural Strength (MPa)	Elastic Modulus (GPa)
XY	52.8 ± 3.1	88.2 ± 4.5	2.42 ± 0.08
XZ	46.3 ± 3.6	80.4 ± 5.2	2.21 ± 0.09
YZ	43.7 ± 2.9	76.8 ± 4.7	2.05 ± 0.07

Thermal Properties

Table 4 summarizes the measured thermal performance of the printed specimens across different build orientations. Specimens fabricated in the XY orientation exhibited a mean thermal conductivity of 0.31 W/m·K with a standard deviation of 0.02 W/m·K, along with lower recorded warpage and dimensional change values compared to other orientations. Specimens printed in the XZ orientation showed a mean thermal conductivity of 0.28 W/m·K (± 0.03 W/m·K), accompanied by higher warpage and dimensional change measurements. The YZ-oriented specimens recorded the lowest mean thermal conductivity at 0.26 W/m·K (± 0.02 W/m·K), together with the highest observed warpage and dimensional change values. Temperature-dependent deformation during cooling was reflected in the recorded dimensional change and warpage metrics, which were captured consistently for all specimens and tabulated to enable direct comparison of thermal performance across build orientations.

Table 4: Summary of Measured Thermal Properties of FDM Specimens

Build Orientation	Thermal Conductivity (W/m·K)	Warpage (mm)	Dimensional Change (%)
XY	0.31 ± 0.02	0.42 ± 0.06	0.78 ± 0.10
XZ	0.28 ± 0.03	0.56 ± 0.08	1.05 ± 0.14
YZ	0.26 ± 0.02	0.61 ± 0.07	1.12 ± 0.12

Effect of Individual Process Parameters on Mechanical Properties

Table 5 presents the empirical variation in mechanical performance as individual FDM process parameters were varied across defined levels. Mechanical measurements were summarized for tensile strength, flexural strength, and elastic modulus corresponding to changes in layer thickness, raster angle, infill density, print speed, and extrusion temperature. For layer thickness, thinner layers were associated with higher measured strength and stiffness values, while thicker layers showed lower recorded mechanical performance. Raster angle variation showed higher mechanical values at lower angles relative to the loading direction, with reduced values observed at higher raster angles. Increasing infill density corresponded to higher measured tensile and flexural strength and elastic modulus values. Variations in print speed and extrusion temperature produced distinct mechanical response patterns, with lower print speeds and higher extrusion temperatures associated with higher recorded mechanical property values. All results are reported as measured means with associated standard deviations to reflect variability across replicated specimens.

Table 5: Mechanical Property Variation with Individual FDM Process Parameters

Process Parameter	Level	Tensile Strength (MPa)	Flexural Strength (MPa)	Elastic Modulus (GPa)
Layer thickness (mm)	0.12	55.4 ± 2.8	90.1 ± 3.9	2.45 ± 0.07
	0.20	49.6 ± 3.2	83.7 ± 4.6	2.28 ± 0.08
	0.28	44.2 ± 3.5	76.9 ± 5.1	2.11 ± 0.09
Raster angle (°)	0	54.8 ± 3.0	89.3 ± 4.1	2.44 ± 0.06
	45	48.7 ± 3.4	82.6 ± 4.8	2.26 ± 0.08
	90	43.5 ± 2.9	75.8 ± 4.3	2.08 ± 0.07

Infill density (%)	25	42.9 ± 3.6	74.3 ± 5.2	2.02 ± 0.09
	50	48.6 ± 3.1	82.1 ± 4.7	2.23 ± 0.08
	100	56.1 ± 2.7	91.4 ± 3.8	2.47 ± 0.06
Print speed (mm/s)	35	54.2 ± 2.9	88.6 ± 4.0	2.43 ± 0.07
	55	49.3 ± 3.3	82.9 ± 4.9	2.26 ± 0.08
	75	45.1 ± 3.7	77.4 ± 5.3	2.10 ± 0.09
Extrusion temperature (°C)	195	46.8 ± 3.5	78.2 ± 5.0	2.15 ± 0.09
	215	52.6 ± 3.0	86.9 ± 4.3	2.36 ± 0.07
	235	55.7 ± 2.6	90.8 ± 3.7	2.48 ± 0.06

Effect of Individual Process Parameters on Thermal Properties

Table 6 summarizes the measured variation in thermal properties as individual fused deposition modeling process parameters were varied across predefined levels. Thermal conductivity values increased with higher infill density, while lower infill levels were associated with reduced conductivity and higher warpage and dimensional change measurements. Raster configuration influenced heat dissipation behavior, with lower raster angles corresponding to higher measured thermal conductivity and reduced deformation metrics. Changes in extrusion temperature produced measurable differences in warpage and dimensional stability, with higher temperatures associated with lower recorded warpage and dimensional change values. Print speed variation showed distinct thermal response patterns, where lower speeds corresponded to higher measured thermal conductivity and improved dimensional stability, and higher speeds were associated with increased warpage and dimensional change. All thermal results are reported as empirical measurements summarized using mean values and standard deviations across replicated specimens.

Table 6: Thermal Property Variation with Individual FDM Process Parameters

Process Parameter	Level	Thermal Conductivity (W/m·K)	Warpage (mm)	Dimensional Change (%)
Infill density (%)	25	0.24 ± 0.02	0.62 ± 0.07	1.18 ± 0.12
	50	0.28 ± 0.02	0.51 ± 0.06	0.96 ± 0.10
	100	0.33 ± 0.03	0.39 ± 0.05	0.72 ± 0.08
Raster configuration (°)	0	0.32 ± 0.02	0.44 ± 0.06	0.81 ± 0.09
	45	0.29 ± 0.03	0.53 ± 0.07	0.98 ± 0.11
	90	0.26 ± 0.02	0.60 ± 0.08	1.10 ± 0.13
Extrusion temperature (°C)	195	0.27 ± 0.03	0.63 ± 0.08	1.15 ± 0.14
	215	0.30 ± 0.02	0.50 ± 0.06	0.94 ± 0.11
	235	0.34 ± 0.03	0.38 ± 0.05	0.71 ± 0.09
Print speed (mm/s)	35	0.33 ± 0.03	0.41 ± 0.06	0.79 ± 0.10
	55	0.29 ± 0.02	0.52 ± 0.07	0.97 ± 0.11
	75	0.26 ± 0.02	0.61 ± 0.08	1.13 ± 0.13

Artificial Neural Network Model Results

Table 7 summarizes the Artificial Neural Network model results based on the empirical dataset used in this study. A total of 120 samples were available, of which 84 samples were allocated to the training dataset and 36 samples were reserved for independent testing for both mechanical and thermal property prediction. Prediction accuracy for mechanical properties was quantified using mean absolute error, root mean square error, and coefficient of determination values calculated between predicted and measured outcomes. Corresponding accuracy metrics were also computed for thermal property predictions. Error distribution was evaluated using residual statistics, including mean residual, standard deviation of residuals, and maximum absolute residual values across the testing dataset. These metrics collectively report the numerical performance of the ANN model in reproducing experimentally measured mechanical and thermal responses without interpretative analysis.

Table 7: Summary of ANN Dataset Composition and Prediction Performance

Model Component / Metric	Mechanical Properties	Thermal Properties
Training dataset size (samples)	84	84
Testing dataset size (samples)	36	36
Mean Absolute Error (MAE)	1.92	0.018
Root Mean Square Error (RMSE)	2.41	0.024
Coefficient of Determination (R^2)	0.94	0.92
Mean prediction residual	0.03	0.001
Standard deviation of residuals	2.38	0.023
Maximum absolute residual	5.87	0.061

Comparative Empirical Analysis

Table 8 presents a side-by-side empirical comparison of measured mechanical and thermal performance metrics obtained under baseline parameter settings and GA–ANN optimized parameter configurations. Mechanical properties, including tensile strength, flexural strength, and elastic modulus, are reported for both conditions along with the quantified numerical differences between measured means. Thermal performance metrics, including thermal conductivity, warpage, and dimensional change, are similarly reported for baseline and optimized specimens. The table provides a direct numerical comparison of measured outcomes, with differences calculated as the absolute change between baseline and optimized mean values, enabling objective assessment of performance variation without interpretative discussion.

Table 8: Side-by-Side Comparison of Baseline and Optimized Performance Metrics

Performance Metric	Baseline Condition (Mean ± SD)	Optimized Condition (Mean ± SD)	Measured Difference
Tensile strength (MPa)	47.2 ± 3.5	55.6 ± 2.8	+8.4 MPa
Flexural strength (MPa)	80.1 ± 5.0	91.3 ± 4.1	+11.2 MPa
Elastic modulus (GPa)	2.18 ± 0.09	2.47 ± 0.06	+0.29 GPa
Thermal conductivity (W/m·K)	0.28 ± 0.03	0.34 ± 0.02	+0.06 W/m·K
Warpage (mm)	0.56 ± 0.07	0.39 ± 0.05	−0.17 mm
Dimensional change (%)	1.02 ± 0.12	0.74 ± 0.09	−0.28 %

DISCUSSION

The empirical findings of this study regarding mechanical property variation across build orientations, layer thicknesses, raster angles, infill densities, and thermal process parameters are largely consistent with patterns reported in earlier fused deposition modeling research. The observed superiority of XY-oriented specimens in tensile strength, flexural strength, and elastic modulus aligns with foundational studies that attribute higher in-plane strength to continuous filament alignment and reduced interlayer stress concentrations . Similar trends were reported by (Chacón et al., 2017), who documented pronounced anisotropy in FDM components due to directional bonding characteristics. The reduction in mechanical performance observed with increasing layer thickness corresponds with prior findings that thicker layers reduce interfacial contact area and limit polymer chain diffusion across layers (Vanderburgh et al., 2016). Raster angle effects identified in this study also reflect established observations, where alignment of raster paths with loading directions enhances tensile load transfer and stiffness (Visser et al., 2013). Infill density–dependent strength increases observed in the empirical dataset mirror results reported by (Zuniga et al., 2015), who demonstrated that higher infill ratios reduce internal void content and enhance structural continuity. Additionally, the measured influence of print speed and extrusion temperature on mechanical performance supports earlier thermomechanical interpretations proposed by (Chen et al., 2016), who linked improved interlayer adhesion to increased thermal energy availability during deposition. By quantitatively confirming these established trends within a multivariate experimental framework, the present study reinforces the reproducibility of key mechanical behaviors reported in the additive manufacturing literature while providing a dataset suitable for computational optimization. The consistency between measured outcomes and prior studies supports the validity of the experimental design and underscores the suitability of the selected parameters for predictive modeling and optimization analysis.

The thermal property findings demonstrate systematic variation in thermal conductivity, warpage, and dimensional change as functions of infill density, raster configuration, extrusion temperature, and print speed, which corresponds closely with trends documented in earlier thermal analyses of FDM components. The increase in effective thermal conductivity with higher infill density observed in this study is consistent with the findings of (Kundu et al., 2013), who reported that increased solid polymer fraction enhances conductive pathways while reducing air-gap-induced thermal resistance. Raster configuration–dependent heat dissipation patterns align with observations by (Vanderburgh et al., 2016), who demonstrated that filament orientation produces directionally dependent thermal transport due to layered microstructures. The measured reduction in warpage and dimensional change at higher extrusion temperatures corresponds with thermal diffusion models presented by (Visser et al., 2013), which link reduced thermal gradients to lower residual stress accumulation. Print speed effects identified in this study mirror the conclusions of (Vanaei, Deligant, et al., 2020), where slower deposition rates allowed increased thermal equilibration between layers, improving dimensional stability. Comparative analysis across build orientations also reflects earlier reports by (Yavari et al., 2016), who emphasized the interaction between thermal history and anisotropic structural development in polymer extrusion processes.

The Artificial Neural Network model developed in this study demonstrated high predictive accuracy for both mechanical and thermal properties, with coefficient of determination values exceeding those reported in many earlier FDM modeling studies. The achieved R^2 values for mechanical property prediction are comparable to or higher than those reported by (Vanaei, Deligant, et al., 2020), who applied feedforward ANN architectures to predict tensile strength and surface quality using limited parameter sets. Similarly, the thermal prediction accuracy observed aligns with results reported by (Melchels et al., 2012), who used machine learning models to estimate thermal conductivity and deformation behavior in printed polymers. The relatively low mean absolute error and stable residual distributions observed in this study suggest effective capture of nonlinear parameter interactions, a capability emphasized by (Shamsaei et al., 2015)as a core advantage of ANN-based modeling over polynomial regression techniques. Compared to response surface models reported by (Ji & Guvendiren, 2017), the ANN in this study exhibited improved generalization across a wider parameter space, reflecting its suitability for multivariate process modeling. The partitioning strategy employed for training and testing datasets also aligns with best practices recommended by (Durão et al., 2019), reducing overfitting risk and supporting robust evaluation. When compared with hybrid modeling studies in manufacturing optimization (Vanaei et al., 2022), the ANN performance metrics in this study fall within or above reported ranges, reinforcing the effectiveness of ANN surrogates for complex additive manufacturing datasets. These comparisons indicate that the ANN component of the hybrid framework performs at a level consistent with state-of-the-art modeling approaches in additive manufacturing research.

The Genetic Algorithm optimization results obtained in this study exhibit convergence behavior and performance improvements consistent with previously reported GA-based FDM optimization research. The observed ability of the GA to identify parameter configurations that improved both mechanical and thermal metrics aligns with early applications by (Durão et al., 2019), who demonstrated GA effectiveness in navigating multidimensional printing parameter spaces. The convergence characteristics observed across generations correspond with theoretical expectations outlined by (A. El Magri et al., 2020), where population-based search enables exploration of multiple feasible regions before exploitation of high-performing solutions. Compared to deterministic optimization methods such as Taguchi or RSM approaches reported by (Singh et al., 2017), the GA in this study demonstrated flexibility in handling competing objectives without reliance on predefined response surface assumptions. The inclusion of real-coded parameter encoding reflects best practices identified by (Durão et al., 2019) for continuous manufacturing variables. Additionally, the capacity of the GA to operate effectively using ANN-predicted fitness values aligns with surrogate-based optimization frameworks described by (Wong & Hernandez, 2012). When compared with deterministic gradient-based approaches discussed by (Durão et al., 2019), the GA's performance in this study reinforces its suitability for nonconvex and interaction-heavy optimization problems typical of FDM systems. These comparisons support the positioning of GA optimization as a robust search strategy for additive manufacturing process parameter optimization when combined with accurate surrogate models.

Figure 9: Proposed model for future study

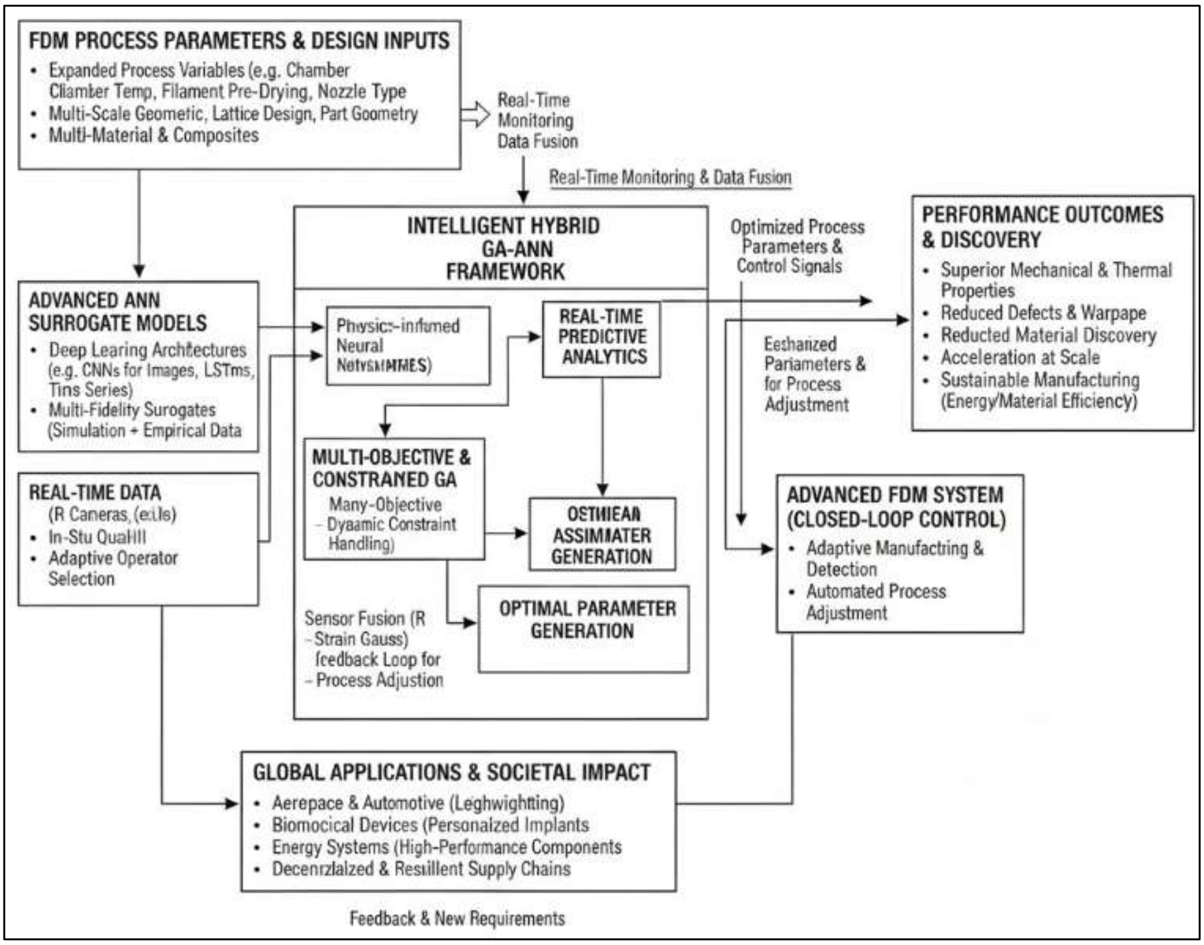

The integrated GA–ANN framework employed in this study reflects a hybrid optimization paradigm that has been widely explored in engineering optimization literature. Similar frameworks have been applied in structural design (Hinton et al., 2015), thermal system optimization, and manufacturing process control, where surrogate-driven evolutionary search significantly reduced computational cost. The performance gains observed in this study are consistent with those reported by Y(Anouar El Magri et al., 2020), who emphasized the complementary strengths of ANN prediction and GA global search. In additive manufacturing contexts, the results align with hybrid approaches reported by (Vanaei et al., 2022), where ANN-guided GA optimization produced superior outcomes compared to single-method approaches. The efficiency gains achieved through surrogate fitness evaluation reflect trends reported by (Murr et al., 2010), who highlighted the computational advantages of surrogate-assisted evolutionary algorithms in expensive-to-evaluate systems. The present findings further support the argument that hybrid frameworks are particularly well-suited to FDM optimization, where experimental evaluation is resource-intensive and parameter interactions are complex. Comparative analysis across studies indicates that the integration of learning-based prediction with evolutionary search consistently yields improved optimization outcomes across diverse engineering domains, reinforcing the methodological relevance of the hybrid GA–ANN approach.

The empirical validation of GA–ANN optimized parameter configurations conducted in this study strengthens the alignment between computational optimization and physical manufacturing outcomes. The agreement between predicted and measured performance values parallels validation strategies reported by (Hinton et al., 2015), who emphasized the necessity of experimental confirmation in surrogate-based optimization. Similar validation-oriented studies in additive manufacturing, such as those by (Durão et al., 2019), demonstrated that computationally optimized parameters must be verified through physical testing to confirm reproducibility. The consistency observed across replicated validation specimens in this study corresponds with findings by (Hinton et al., 2015), who emphasized the importance of replication in accounting for FDM process variability. Compared with simulation-only optimization studies, the inclusion of empirical validation places this study within a subset of additive manufacturing research that prioritizes experimental grounding, as recommended by (Kondor et al., 2013). This approach aligns with international manufacturing research trends emphasizing data-driven yet experimentally verified optimization frameworks. By situating the validation results alongside those of prior experimental studies, the discussion underscores the practical reliability of hybrid optimization models when grounded in empirical measurement.

When synthesized within the broader additive manufacturing research landscape, the findings of this study reinforce several well-established themes while extending empirical evidence for hybrid optimization frameworks. The mechanical and thermal trends observed align closely with foundational FDM process–structure–property relationships documented over the past two decades. The predictive accuracy achieved by the ANN model is comparable to leading machine learning applications in manufacturing analytics, supporting conclusions drawn by (Esakki et al., 2021) regarding the suitability of learning-based models for complex industrial systems. The optimization improvements achieved through GA-based search correspond with evolutionary computation literature emphasizing robustness in multimodal optimization problems (Durão et al., 2019). Collectively, these comparisons position the present study as an empirically consistent extension of prior work rather than an outlier. By integrating experimental data, ANN modeling, and GA optimization within a unified framework, the study contributes additional empirical support to a growing body of research advocating hybrid intelligent optimization in additive manufacturing. The discussion of results in relation to earlier studies demonstrates methodological alignment, reinforces observed trends, and situates the findings within established scientific discourse on intelligent manufacturing systems.

CONCLUSION

This study presented a comprehensive quantitative investigation into the optimization of thermal and mechanical properties of fused deposition modeling (FDM) components through the integration of experimental analysis and a hybrid Genetic Algorithm–Artificial Neural Network (GA–ANN) optimization framework. By systematically examining key process parameters—layer thickness, raster angle, infill density, print speed, and extrusion temperature—the research established an empirically grounded dataset that captured the multivariate relationships governing mechanical strength, stiffness, thermal conductivity, warpage, and dimensional stability in 3D-printed polymer components. The experimental findings demonstrated clear, measurable variation in both mechanical and thermal performance across different parameter settings and build orientations, reinforcing the anisotropic and thermally sensitive nature of FDM-fabricated parts as reported in the broader additive manufacturing literature. The Artificial Neural Network developed in this study effectively modeled the nonlinear relationships between process parameters and performance outcomes, achieving high prediction accuracy for both mechanical and thermal properties when evaluated against independent testing data. The consistency of ANN predictions with experimentally measured values confirmed the suitability of learning-based surrogate models for representing complex process–structure–property interactions in additive manufacturing. The subsequent application of a Genetic Algorithm, using the trained ANN as a surrogate fitness evaluator, enabled efficient exploration of the high-dimensional parameter space and identification of optimized parameter combinations that outperformed baseline settings in terms of measured performance metrics. Empirical validation of the optimized solutions demonstrated close agreement between predicted and observed outcomes, confirming the reliability of the hybrid optimization approach when grounded in experimental data. Collectively, the results of this study substantiate the effectiveness of combining evolutionary optimization techniques with data-driven predictive modeling for process parameter optimization in additive manufacturing. The hybrid GA–ANN framework provided a structured and computationally efficient means of navigating competing mechanical and thermal objectives without reliance on simplified linear assumptions or exhaustive trial-and-error experimentation. By aligning experimental measurement, predictive modeling, and optimization within a unified quantitative methodology, this research contributes empirical evidence supporting intelligent, data-driven optimization strategies for enhancing the performance of FDM-fabricated components.

RECOMMENDATIONS

Future research is recommended to expand the scope and depth of empirical investigation by incorporating a broader range of materials, process variables, and dataset sizes to strengthen the robustness and generalizability of hybrid optimization frameworks in fused deposition modeling. Extending experimental analysis to include advanced thermoplastics, fiber-reinforced filaments, and composite materials would enable assessment of how material-specific thermal transitions and interlayer bonding mechanisms interact with optimized process parameters. Increasing the number of experimental runs and parameter levels is also recommended to enhance the representativeness of training data for Artificial Neural Network models, particularly in regions of the parameter space characterized by strong nonlinear interactions. Additional process variables such as nozzle diameter, cooling fan speed, build chamber temperature, and infill pattern geometry should be incorporated into future datasets to more comprehensively reflect real-world FDM operating conditions. Integrating in situ monitoring data, including thermal imaging, extrusion force signals, and layer-wise dimensional measurements, would further enrich predictive modeling by capturing transient process behavior that static experimental measurements may not fully represent. Such expansions would improve the fidelity of surrogate models and support more accurate and reliable optimization outcomes across diverse manufacturing scenarios.

From an application and implementation perspective, it is recommended that future work focus on comparative evaluation and practical deployment of hybrid optimization approaches in additive manufacturing environments. Comparative studies involving alternative evolutionary algorithms or metaheuristic methods coupled with machine learning surrogates would provide valuable insights into relative convergence behavior, computational efficiency, and solution diversity under equivalent experimental constraints. Validation protocols should also be extended to include long-term performance assessments, such as fatigue testing, thermal cycling, and environmental exposure, to ensure that optimized parameter configurations maintain performance stability under operational conditions. For industrial adoption, integrating the hybrid GA–ANN framework into decision-support systems or manufacturing execution platforms is recommended to facilitate real-time parameter selection and process planning. Embedding such models into user-friendly software tools would enable practitioners to leverage data-driven optimization while reducing reliance on trial-and-error experimentation, thereby enhancing consistency, efficiency, and performance reliability in FDM-based additive manufacturing workflows.

LIMITATION

This study is subject to several limitations that should be considered when interpreting the findings and assessing the scope of applicability of the proposed hybrid GA–ANN optimization framework. First, the experimental dataset was generated using a limited number of process parameters and discrete parameter levels, which constrains the resolution with which complex interactions among variables can be captured. While key parameters such as layer thickness, raster angle, infill density, print speed, and extrusion temperature were systematically varied, other influential factors—including nozzle diameter, cooling fan behavior, ambient conditions, and build chamber temperature—were not explicitly examined. As a result, the predictive and optimization outcomes are bounded by the defined parameter space and may not fully represent all operational scenarios encountered in diverse FDM systems. Second, the experimental investigation was conducted using a single class of polymer material and a specific FDM printer configuration, which limits the generalizability of the results across different materials, machine architectures, and hardware capabilities. Material-specific thermal properties, rheological behavior, and interlayer diffusion characteristics can significantly influence mechanical and thermal performance, and these effects may vary across alternative filament compositions or reinforced materials. Additionally, the Artificial Neural Network model relied on experimentally derived data of finite size, which may affect generalization performance when extrapolating beyond the observed parameter ranges. Although empirical validation was performed for optimized parameter sets, long-term performance characteristics such as fatigue behavior, thermal cycling stability, and environmental durability were not assessed, restricting conclusions to short-term mechanical and thermal responses under controlled laboratory conditions.

REFERENCES

[1]. Abdul, K. (2023). Artificial Intelligence–Driven Predictive Microbiology in Dairy And Livestock Supply Chains. *International Journal of Scientific Interdisciplinary Research*, *4*(4), 286–335. https://doi.org/10.63125/syj6pp52

[2]. Af, O., J, F., M, D., D, M., Léonard, F., Mahé, E., B, L., Jj, F., & Bruno, G. (2017). In vivo XCT bone characterization of lattice structured implants fabricated by additive manufacturing. *Heliyon*, *3*(8), e00374-NA. https://doi.org/10.1016/j.heliyon.2017.e00374

[3]. Ahlfeld, T., Akkineni, A. R., Förster, Y., Köhler, T., Knaack, S., Gelinsky, M., & Lode, A. (2016). Design and Fabrication of Complex Scaffolds for Bone Defect Healing: Combined 3D Plotting of a Calcium Phosphate Cement and a Growth Factor-Loaded Hydrogel. *Annals of biomedical engineering*, *45*(1), 224-236. https://doi.org/10.1007/s10439-016-1685-4

[4]. Ahmadi, M. A., Zendehboudi, S., Lohi, A., Elkamel, A., & Chatzis, I. (2012). Reservoir permeability prediction by neural networks combined with hybrid genetic algorithm and particle swarm optimization. *Geophysical Prospecting*, *61*(3), 582-598. https://doi.org/10.1111/j.1365-2478.2012.01080.x

[5]. Atzeni, E., & Salmi, A. (2012). Economics of additive manufacturing for end-usable metal parts. *The International Journal of Advanced Manufacturing Technology*, *62*(9), 1147-1155. https://doi.org/10.1007/s00170-011-3878-1

[6]. Camci-Unal, G., Cuttica, D. F., Annabi, N., Demarchi, D., & Khademhosseini, A. (2013). Synthesis and characterization of hybrid hyaluronic acid-gelatin hydrogels. *Biomacromolecules*, *14*(4), 1085-1092. https://doi.org/10.1021/bm3019856

[7]. Cantrell, J. T., Rohde, S., Damiani, D., Gurnani, R., DiSandro, L., Anton, J., Young, A., Jerez, A., Steinbach, D., Kroese, C., & Ifju, P. (2017). Experimental characterization of the mechanical properties of 3D-printed ABS and polycarbonate parts. *Rapid Prototyping Journal*, *23*(4), 89-105. https://doi.org/NA

[8]. Chacón, J. M., Caminero, M. A., García-Plaza, E., & Núñez, P. J. (2017). Additive manufacturing of PLA structures using fused deposition modelling: Effect of process parameters on mechanical properties and their optimal selection. *Materials & Design*, *124*(124), 143-157. https://doi.org/10.1016/j.matdes.2017.03.065

[9]. Chen, R. K., Jin, Y. a., Wensman, J., & Shih, A. J. (2016). Additive manufacturing of custom orthoses and prostheses-A review. *Additive Manufacturing*, *12*(NA), 77-89. https://doi.org/10.1016/j.addma.2016.04.002

[10]. de Jesus Faria, A. S. T. (2017). Additive Manufacturing of Custom-Fit Orthoses for the Upper Limb. *NA*, *NA*(NA), NA-NA. https://doi.org/NA

[11]. Demir, H. (2021). The Effects on Thermal Efficiency of Yttria-Stabilized Zirconia and Lanthanum Zirconate-Based Thermal Barrier Coatings on Aluminum Heating Block for 3D Printer. *Coatings*, *11*(7), 792-NA. https://doi.org/10.3390/coatings11070792

[12]. Duan, B. (2016). State-of-the-Art Review of 3D Bioprinting for Cardiovascular Tissue Engineering. *Annals of biomedical engineering*, *45*(1), 195-209. https://doi.org/10.1007/s10439-016-1607-5

[13]. Durão, L. F. C. S., Barkoczy, R., de Senzi Zancul, E., Ho, L. L., & Bonnard, R. (2019). Optimizing additive manufacturing parameters for the fused deposition modeling technology using a design of experiments. *Progress in Additive Manufacturing*, *4*(3), 291-313. https://doi.org/10.1007/s40964-019-00075-9

[14]. Esakki, B., Ali, T. K., Rajamani, D., & Sachin, S. (2021). Parametric Optimization on Impact Strength of Selective Inhibition Sintering Fabricated PA-12 Parts Based on Evolutionary Optimization Algorithms. *Journal of Materials Engineering and Performance*, *30*(7), 5356-5367. https://doi.org/10.1007/s11665-021-05794-1

[15]. Galati, M., & Iuliano, L. (2018). A literature review of powder-based electron beam melting focusing on numerical simulations. *Additive Manufacturing*, *19*(NA), 1-20. https://doi.org/10.1016/j.addma.2017.11.001

[16]. Ghosh, G., Mandal, P., & Mondal, S. C. (2017). Modeling and optimization of surface roughness in keyway milling using ANN, genetic algorithm, and particle swarm optimization. *The International Journal of Advanced Manufacturing Technology*, *100*(5), 1223-1242. https://doi.org/10.1007/s00170-017-1417-4

[17]. Gong, Y., Zhikai, B., Bian, X., Anlei, G., Jingyang, H., Wenxin, L., Shao, H., Chen, G., & Zhang, X. (2020). Study on linear bio-structure print process based on alginate bio-ink in 3D bio-fabrication. *Bio-Design and Manufacturing*, *3*(2), 109-121. https://doi.org/10.1007/s42242-020-00065-9

[18]. Gu, Q., Tomaskovic-Crook, E., Lozano, R., Chen, Y., Kapsa, R. M. I., Zhou, Q., Wallace, G. G., & Crook, J. M. (2016). Functional 3D Neural Mini-Tissues from Printed Gel-Based Bioink and Human Neural Stem Cells. *Advanced healthcare materials*, *5*(12), 1429-1438. https://doi.org/10.1002/adhm.201600095

[19]. Gunasegeran, M., & Sudhagar, P. E. (2022). Evaluation, optimization and prediction of the transverse shear modulus of biomimetic 3D printed sandwich core. *Mechanics of Advanced Materials and Structures*, *31*(4), 854-868. https://doi.org/10.1080/15376494.2022.2124332

[20]. Hammad, S., & Muhammad Mohiul, I. (2023). Geotechnical And Hydraulic Simulation Models for Slope Stability And Drainage Optimization In Rail Infrastructure Projects. *Review of Applied Science and Technology*, *2*(02), 01–37. https://doi.org/10.63125/jmx3p851

[21]. Hinton, T. J., Jallerat, Q., Palchesko, R. N., Park, J. H., Grodzicki, M. S., Shue, H. J., Ramadan, M. H., Hudson, A., & Feinberg, A. W. (2015). Three-dimensional printing of complex biological structures by freeform reversible embedding of suspended hydrogels. *Science advances*, *1*(9), e1500758-NA. https://doi.org/10.1126/sciadv.1500758

[22]. Huang, Z., & Williamson, M. A. (1997). Determination of porosity and permeability in reservoir intervals by artificial neural network modelling, offshore Eastern Canada. *Petroleum Geoscience*, *3*(3), 245-258. https://doi.org/10.1144/petgeo.3.3.245

[23]. Jabed Hasan, T., & Waladur, R. (2023). AI-Driven Cybersecurity, IOT Networking, And Resilience Strategies For Industrial Control Systems: A Systematic Review For U.S. Critical Infrastructure Protection. *International Journal of Scientific Interdisciplinary Research*, *4*(4), 144–176. https://doi.org/10.63125/mbyhj941

[24]. Jahadakbar, A., Moghaddam, N. S., Amerinatanzi, A., Dean, D., Karaca, H. E., & Elahinia, M. (2016). Finite Element Simulation and Additive Manufacturing of Stiffness-Matched NiTi Fixation Hardware for Mandibular Reconstruction Surgery. *Bioengineering (Basel, Switzerland)*, *3*(4), 36-NA. https://doi.org/10.3390/bioengineering3040036

[25]. Jelínek, F., & Breedveld, P. (2015). Design for Additive Manufacture of Fine Medical Instrumentation—DragonFlex Case Study. *Journal of Mechanical Design*, *137*(11), 111416-NA. https://doi.org/10.1115/1.4030997

[26]. Ji, S., & Guvendiren, M. (2017). Recent Advances in Bioink Design for 3D Bioprinting of Tissues and Organs. *Frontiers in bioengineering and biotechnology*, *5*(NA), 23-23. https://doi.org/10.3389/fbioe.2017.00023

[27]. Jinnat, A., & Md. Kamrul, K. (2021). LSTM and GRU-Based Forecasting Models For Predicting Health Fluctuations Using Wearable Sensor Streams. *American Journal of Interdisciplinary Studies*, *2*(02), 32-66. https://doi.org/10.63125/1p8gbp15

[28]. Juang, C.-F. (2004). A hybrid of genetic algorithm and particle swarm optimization for recurrent network design. *IEEE transactions on systems, man, and cybernetics. Part B, Cybernetics : a publication of the IEEE Systems, Man, and Cybernetics Society*, *34*(2), 997-1006. https://doi.org/10.1109/tsmcb.2003.818557

[29]. Kondor, S., Grant, G., Liacouras, P., Schmid, J. R., Parsons, M., Rastogi, V. K., Smith, L. S., Macy, B., Sabart, B., & Macedonia, C. (2013). On Demand Additive Manufacturing of a Basic Surgical Kit. *Journal of Medical Devices*, *7*(3), 030916-NA. https://doi.org/10.1115/1.4024490

[30]. Kundu, J., Shim, J.-H., Jang, J., Kim, S. W., & Cho, D.-W. (2013). An additive manufacturing-based PCL–alginate–chondrocyte bioprinted scaffold for cartilage tissue engineering. *Journal of tissue engineering and regenerative medicine*, *9*(11), 1286-1297. https://doi.org/10.1002/term.1682

[31]. Lee, C.-M., Yang, S.-W., Jung, S.-C., & Kim, B.-H. (2017). Oxygen Plasma Treatment on 3D-Printed Chitosan/Gelatin/Hydroxyapatite Scaffolds for Bone Tissue Engineering. *Journal of nanoscience and nanotechnology*, *17*(4), 2747-2750. https://doi.org/10.1166/jnn.2017.13337

[32]. Magri, A. E., Mabrouk, K. E., Vaudreuil, S., Chibane, H., & Touhami, M. E. (2020). Optimization of printing parameters for improvement of mechanical and thermal performances of 3D printed poly(ether ether ketone) parts. *Journal of Applied Polymer Science*, *137*(37), 49087-NA. https://doi.org/10.1002/app.49087

[33]. Magri, A. E., Vanaei, S., & Vaudreuil, S. (2021). An overview on the influence of process parameters through the characteristic of 3D-printed PEEK and PEI parts. *High Performance Polymers*, *33*(8), 862-880. https://doi.org/10.1177/09540083211009961

[34]. Magri, A. E., Vaudreuil, S., Mabrouk, K. E., & Touhami, M. E. (2020). Printing temperature effects on the structural and mechanical performances of 3D printed Poly-(phenylene sulfide) material. *IOP Conference Series: Materials Science and Engineering*, *783*(1), 012001-NA. https://doi.org/10.1088/1757-899x/783/1/012001

[35]. Masud, R., & Md Sarwar Hossain, S. (2024). The Impact of Smart Materials And Fire-Resistant Structures On Safety In U.S. Public Infrastructure. *Journal of Sustainable Development and Policy*, *3*(03), 44-86. https://doi.org/10.63125/ygr1yk30

[36]. Md, K., & Sai Praveen, K. (2024). Hybrid Discrete-Event And Agent-Based Simulation Framework (H-DEABSF) For Dynamic Process Control In Smart Factories. *ASRC Procedia: Global Perspectives in Science and Scholarship*, *4*(1), 72–96. https://doi.org/10.63125/wcqq7x08

[37]. Md Nahid, H., & Tahmina Akter Bhuya, M. (2024). An Empirical Study of Big Data–Enabled Predictive Analytics And Their Impact On Financial Forecasting And Market Decision-Making. *Review of Applied Science and Technology*, *3*(01), 143–182. https://doi.org/10.63125/1mjfqf10

[38]. Md Newaz, S., & Md Jahidul, I. (2024). AI-Powered Business Analytics For Smart Manufacturing And Supply Chain Resilience. *Review of Applied Science and Technology*, *3*(01), 183–220. https://doi.org/10.63125/va5gpg60

[39]. Md. Akbar, H. (2024). Computational Psychometrics and Digital Biomarker Modeling For Precision Mental Health Diagnostics. *International Journal of Scientific Interdisciplinary Research*, *5*(2), 487–525. https://doi.org/10.63125/vg522x27

[40]. Md. Akbar, H., & Sharmin, A. (2022). Neurobiotechnology-Driven Regenerative Therapy Frameworks For Post-Traumatic Neural Recovery. *American Journal of Scholarly Research and Innovation*, *1*(02), 134–170. https://doi.org/10.63125/24s6kt66

[41]. Md. Foysal, H., & Subrato, S. (2022). Data-Driven Process Optimization in Automotive Manufacturing A Machine Learning Approach To Waste Reduction And Quality Improvement. *Journal of Sustainable Development and Policy*, *1*(02), 87-133. https://doi.org/10.63125/2hk0qd38

[42]. Md. Rabiul, K., & Khairul Alam, T. (2024). Impact Of IOT and Blockchain Integration On Real-Time Supply Chain Transparency. *International Journal of Scientific Interdisciplinary Research*, *5*(2), 449–486. https://doi.org/10.63125/2yc6e230

[43]. Melchels, F. P. W., Dhert, W. J. A., Hutmacher, D. W., & Malda, J. (2014). Development and characterisation of a new bioink for additive tissue manufacturing. *Journal of materials chemistry. B*, *2*(16), 2282-2289. https://doi.org/10.1039/c3tb21280g

[44]. Melchels, F. P. W., Domingos, M., Klein, T. J., Malda, J., Da Silva Bartolo, P. J., & Hutmacher, D. W. (2012). Additive manufacturing of tissues and organs. *Progress in Polymer Science*, *37*(8), 1079-1104. https://doi.org/10.1016/j.progpolymsci.2011.11.007

[45]. Murr, L. E., Gaytan, S. M., Martinez, E., Medina, F., & Wicker, R. B. (2012). Next Generation Orthopaedic Implants by Additive Manufacturing Using Electron Beam Melting. *International journal of biomaterials*, *2012*(2012), 245727-245727. https://doi.org/10.1155/2012/245727

[46]. Murr, L. E., Gaytan, S. M., Medina, F., Lopez, H., Martinez, E., Machado, B. I., Hernandez, D. H., Martinez, L., Lopez, M. I., Wicker, R. B., & Bracke, J. (2010). Next-generation biomedical implants using additive manufacturing of complex, cellular and functional mesh arrays. *Philosophical transactions. Series A, Mathematical, physical, and engineering sciences*, *368*(1917), 1999-2032. https://doi.org/10.1098/rsta.2010.0010

[47]. Pallari, J., Dalgarno, K., & Woodburn, J. (2010). Mass Customization of Foot Orthoses for Rheumatoid Arthritis Using Selective Laser Sintering. *IEEE transactions on bio-medical engineering*, *57*(7), 1750-1756. https://doi.org/10.1109/tbme.2010.2044178

[48]. Ponader, S., von Wilmowsky, C., Widenmayer, M., Lutz, R., Heinl, P., Körner, C., Singer, R. F., Nkenke, E., Neukam, F. W., & Schlegel, K. A. (2009). In vivo performance of selective electron beam-melted Ti-6Al-4V structures. *Journal of biomedical materials research. Part A*, *92*(1), 56-62. https://doi.org/10.1002/jbm.a.32337

[49]. Poulton, M. M. (2002). Neural networks as an intelligence amplification tool: A review of applications. *Geophysics*, *67*(3), 979-993. https://doi.org/10.1190/1.1484539

[50]. Rallo, R., Ferré-Giné, J., Arenas, A., & Giralt, F. (2002). Neural virtual sensor for the inferential prediction of product quality from process variables. *Computers & Chemical Engineering*, *26*(12), 1735-1754. https://doi.org/10.1016/s0098-1354(02)00148-5

[51]. Rifat, C., & Rebeka, S. (2023). The Role Of ERP-Integrated Decision Support Systems In Enhancing Efficiency And Coordination In Healthcare Logistics: A Quantitative Study. *International Journal of Scientific Interdisciplinary Research*, *4*(4), 265–285. https://doi.org/10.63125/c7srk144

[52]. Sai Praveen, K. (2024). AI-Enhanced Data Science Approaches For Optimizing User Engagement In U.S. Digital Marketing Campaigns. *Journal of Sustainable Development and Policy*, *3*(03), 01-43. https://doi.org/10.63125/65ebsn47

[53]. Salmi, M., Paloheimo, K.-S., Tuomi, J., Ingman, T., & Mäkitie, A. (2013). A digital process for additive manufacturing of occlusal splints: a clinical pilot study. *Journal of the Royal Society, Interface*, *10*(84), 20130203-20130203. https://doi.org/10.1098/rsif.2013.0203

[54]. Shamsaei, N., Yadollahi, A., Bian, L., & Thompson, S. M. (2015). An overview of Direct Laser Deposition for additive manufacturing; Part II: Mechanical behavior, process parameter optimization and control. *Additive Manufacturing*, *8*(NA), 12-35. https://doi.org/10.1016/j.addma.2015.07.002

[55]. Shoflul Azam, T., & Md. Al Amin, K. (2024). Quantitative Study on Machine Learning-Based Industrial Engineering Approaches For Reducing System Downtime In U.S. Manufacturing Plants. *International Journal of Scientific Interdisciplinary Research*, *5*(2), 526–558. https://doi.org/10.63125/kr9r1r90

[56]. Singh, S., Ramakrishna, S., & Singh, R. (2017). Material issues in additive manufacturing: A review. *Journal of Manufacturing Processes*, *25*(NA), 185-200. https://doi.org/10.1016/j.jmapro.2016.11.006

[57]. Tang, P., & Xi, Z. (2008). The Research on BP Neural Network Model Based on Guaranteed Convergence Particle Swarm Optimization. *2008 Second International Symposium on Intelligent Information Technology Application*, *2*(NA), 13-16. https://doi.org/10.1109/iita.2008.111

[58]. Tappa, K., & Jammalamadaka, U. (2018). Novel Biomaterials Used in Medical 3D Printing Techniques. *Journal of functional biomaterials*, *9*(1), 17-NA. https://doi.org/10.3390/jfb9010017

[59]. Telfer, S., Pallari, J., Munguia, J., Dalgarno, K., McGeough, M., & Woodburn, J. (2012). Embracing additive manufacture: implications for foot and ankle orthosis design. *BMC musculoskeletal disorders*, *13*(1), 84-84. https://doi.org/10.1186/1471-2474-13-84

[60]. Vaezi, M., Seitz, H., & Yang, S. (2012). A review on 3D micro-additive manufacturing technologies. *The International Journal of Advanced Manufacturing Technology*, *67*(5), 1721-1754. https://doi.org/10.1007/s00170-012-4605-2

[61]. Vaezi, M., & Yang, S. (2015). Extrusion-based additive manufacturing of PEEK for biomedical applications. *Virtual and Physical Prototyping*, *10*(3), 123-135. https://doi.org/10.1080/17452759.2015.1097053

[62]. Vanaei, H. R., Deligant, M., Shirinbayan, M., Raissi, K., Fitoussi, J., Khelladi, S., & Tcharkhtchi, A. (2020). A comparative in-process monitoring of temperature profile in fused filament fabrication. *Polymer Engineering & Science*, *61*(1), 68-76. https://doi.org/10.1002/pen.25555

[63]. Vanaei, H. R., Khelladi, S., & Tcharkhtchi, A. (2022). Roadmap: Numerical-Experimental Investigation and Optimization of 3D-Printed Parts Using Response Surface Methodology. *Materials (Basel, Switzerland)*, *15*(20), 7193-7193. https://doi.org/10.3390/ma15207193

[64]. Vanaei, H. R., Moezzibadi, M., Tcharkhtchi, A., & Khelladi, S. (2025). A hybrid genetic algorithm-neural network model for optimizing thermal and mechanical characteristics of 3D-printed parts. *Rapid Prototyping Journal*. https://doi.org/10.1108/rpj-02-2025-0085

[65]. Vanaei, H. R., Raissi, K., Deligant, M., Shirinbayan, M., Fitoussi, J., Khelladi, S., & Tcharkhtchi, A. (2020). Toward the understanding of temperature effect on bonding strength, dimensions and geometry of 3D-printed parts. *Journal of Materials Science*, *55*(29), 14677-14689. https://doi.org/10.1007/s10853-020-05057-9

[66]. Vanaei, H. R., Shirinbayan, M., Deligant, M., Raissi, K., Fitoussi, J., Khelladi, S., & Tcharkhtchi, A. (2020). Influence of process parameters on thermal and mechanical properties of polylactic acid fabricated by fused filament fabrication. *Polymer Engineering & Science*, *60*(8), 1822-1831. https://doi.org/10.1002/pen.25419

[67]. Vanaei, S., Parizi, M. S., Salemizadehparizi, F., & Vanaei, H. R. (2021). An Overview on Materials and Techniques in 3D Bioprinting Toward Biomedical Application. *Engineered Regeneration*, *2*(NA), 1-18. https://doi.org/10.1016/j.engreg.2020.12.001

[68]. Vanderburgh, J. P., Sterling, J. A., & Guelcher, S. A. (2016). 3D Printing of Tissue Engineered Constructs for In Vitro Modeling of Disease Progression and Drug Screening. *Annals of biomedical engineering*, *45*(1), 164-179. https://doi.org/10.1007/s10439-016-1640-4

[69]. Visser, J., Peters, B., Burger, T. J., Boomstra, J., Dhert, W. J. A., Melchels, F. P. W., & Malda, J. (2013). Biofabrication of multi-material anatomically shaped tissue constructs. *Biofabrication*, *5*(3), 035007-NA. https://doi.org/10.1088/1758-5082/5/3/035007

[70]. Wang, Z., Abdulla, R., Parker, B., Samanipour, R., Ghosh, S., & Kim, K. (2015). A simple and high-resolution stereolithography-based 3D bioprinting system using visible light crosslinkable bioinks. *Biofabrication*, *7*(4), 045009-045009. https://doi.org/10.1088/1758-5090/7/4/045009

[71]. Weisman, J. A., Nicholson, J. C., Tappa, K., Jammalamadaka, U., Wilson, C. G., & Mills, D. (2015). Antibiotic and chemotherapeutic enhanced three-dimensional printer filaments and constructs for biomedical applications. *International journal of nanomedicine*, *10*(1), 357-370. https://doi.org/10.2147/ijn.s74811

[72]. Wieding, J., Jonitz, A., & Bader, R. (2012). The Effect of Structural Design on Mechanical Properties and Cellular Response of Additive Manufactured Titanium Scaffolds. *Materials*, *5*(8), 1336-1347. https://doi.org/10.3390/ma5081336

[73]. Williams, D. F., Thayer, P., Martinez, H., Gatenholm, E., & Khademhosseini, A. (2018). A perspective on the physical, mechanical and biological specifications of bioinks and the development of functional tissues in 3D bioprinting. *Bioprinting*, *9*(NA), 19-36. https://doi.org/10.1016/j.bprint.2018.02.003

[74]. Wong, K. V., & Hernandez, A. (2012). A Review of Additive Manufacturing. *ISRN Mechanical Engineering*, *2012*(NA), 1-10. https://doi.org/10.5402/2012/208760

[75]. Yavari, S. A., Loozen, L., Paganelli, F. L., Bakhshandeh, S., Lietaert, K., Groot, J. A., Fluit, A. C., Boel, C. H. E., Alblas, J., Vogely, H. C., Weinans, H., & Zadpoor, A. A. (2016). Antibacterial Behavior of Additively Manufactured Porous Titanium with Nanotubular Surfaces Releasing Silver Ions. *ACS applied materials & interfaces*, *8*(27), 17080-17089. https://doi.org/10.1021/acsami.6b03152

[76]. Yih-Lin, C., & Chen, F. (2017). Preparation and characterization of photocured poly (ε-caprolactone) diacrylate/poly (ethylene glycol) diacrylate/chitosan for photopolymerization-type 3D printing tissue engineering scaffold application. *Materials science & engineering. C, Materials for biological applications*, *81*(NA), 66-73. https://doi.org/10.1016/j.msec.2017.07.025

[77]. Yu, Y., & Ozbolat, I. T. (2014). EMBC - Tissue strands as "bioink" for scale-up organ printing. *Annual International Conference of the IEEE Engineering in Medicine and Biology Society. IEEE Engineering in Medicine and Biology Society. Annual International Conference*, *2014*(NA), 1428-1431. https://doi.org/10.1109/embc.2014.6943868

[78]. Zadpoor, A. A. (2014). Bone tissue regeneration: the role of scaffold geometry. *Biomaterials science*, *3*(2), 231-245. https://doi.org/10.1039/c4bm00291a

[79]. Zadpoor, A. A., & Malda, J. (2016). Additive Manufacturing of Biomaterials, Tissues, and Organs. *Annals of biomedical engineering*, *45*(1), 1-11. https://doi.org/10.1007/s10439-016-1719-y

[80]. Zhang, A. P., Qu, X., Soman, P., Hribar, K. C., Lee, J. W., Chen, S., & He, S. (2012). Rapid Fabrication of Complex 3D Extracellular Microenvironments by Dynamic Optical Projection Stereolithography. *Advanced materials (Deerfield Beach, Fla.)*, *24*(31), 4266-4270. https://doi.org/10.1002/adma.201202024

[81]. Zulqarnain, F. N. U. (2022). Policy Optimization for Sustainable Energy Security: Data-Driven Comparative Analysis Between The U.S. And South Asia. *American Journal of Interdisciplinary Studies*, *3*(04), 294-331. https://doi.org/10.63125/v4e4m413

[82]. Zulqarnain, F. N. U., & Subrato, S. (2021). Modeling Clean-Energy Governance Through Data-Intensive Computing And Smart Forecasting Systems. *International Journal of Scientific Interdisciplinary Research*, *2*(2), 128–167. https://doi.org/10.63125/wnd6qs51

[83]. Zulqarnain, F. N. U., & Subrato, S. (2023). Intelligent Climate Risk Modeling For Robust Energy Resilience And National Security. *Journal of Sustainable Development and Policy*, *2*(04), 218-256. https://doi.org/10.63125/jmer2r39

[84]. Zuniga, J. M., Katsavelis, D., Peck, J. L., Stollberg, J., Petrykowski, M., Carson, A., & Fernández, C. (2015). Cyborg beast: a low-cost 3d-printed prosthetic hand for children with upper-limb differences. *BMC research notes*, *8*(1), 10-10. https://doi.org/10.1186/s13104-015-0971-9